NASA TECHNICAL MEMORANDUM

NASA TM X-2472

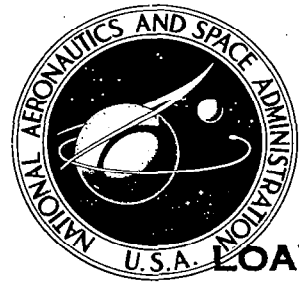

NASA TM X-2472

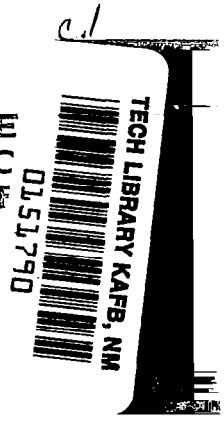

EXPERIMENTAL HEAT TRANSFER AND FLOW RESULTS OF A CHORDWISE-FINNED TURBINE VANE WITH IMPINGEMENT, FILM, AND CONVECTION COOLING

by James W. Gauntner, Jan M. Lane, Robert P. Dengler, and Robert O. Hickel

Lewis Research Center and
U.S. Army Air Mobility R&D Laboratory
Cleveland, Ohio 44135

NATIONAL AERONAUTICS AND SPACE ADMINISTRATION • WASHINGTON, D. C. • APRIL 1972

1. Report No.	2. Government Accession No.	3. Recipient's Catalog No.
NASA TM X-2472		

4. Title and Subtitle	5. Report Date
EXPERIMENTAL HEAT TRANSFER AND FLOW RESULTS OF A CHORDWISE-FINNED TURBINE VANE WITH IMPINGEMENT, FILM, AND CONVECTION COOLING	April 1972
	6. Performing Organization Code
7. Author(s)	8. Performing Organization Report No.
James W. Gauntner, Jan M. Lane, Robert P. Dengler, and Robert O. Hickel	E-6547
	10. Work Unit No.
9. Performing Organization Name and Address	764-74
NASA Lewis Research Center and U.S. Army Air Mobility R&D Laboratory Cleveland, Ohio 44135	11. Contract or Grant No.
	13. Type of Report and Period Covered
12. Sponsoring Agency Name and Address	Technical Memorandum
National Aeronautics and Space Administration Washington, D. C. 20546	14. Sponsoring Agency Code

15. Supplementary Notes

16. Abstract

Experimental heat transfer data are presented for a vane tested in a turbojet engine at turbine inlet gas temperatures to 1644 K (2500° F), coolant temperatures to 700 K (800° F), and coolant-to-gas flow ratios to 0.187. Methods are presented for correlating the heat transfer data and obtaining the coolant flow distribution through the vane. Calculated and measured coolant flow distributions and vane metal temperatures are compared.

17. Key Words (Suggested by Author(s))	18. Distribution Statement
Cooled turbine vane design; High temperature turbojet engine; Coolant flow distribution; Gas pressure distribution; Heat transfer	Unclassified - unlimited

19. Security Classif. (of this report)	20. Security Classif. (of this page)	21. No. of Pages	22. Price*
Unclassified	Unclassified	62	$3.00

* For sale by the National Technical Information Service, Springfield, Virginia 22151

CONTENTS

EXPERIMENTAL HEAT TRANSFER AND FLOW RESULTS OF A CHORDWISE-FINNED TURBINE VANE WITH IMPINGEMENT, FILM, AND CONVECTION COOLING

by James W. Gauntner, Jan M. Lane, Robert P. Dengler, and Robert O. Hickel

Lewis Research Center and
U. S. Army Air Mobility R&D Laboratory

SUMMARY

An experimental investigation is discussed, and the data presented, for the heat transfer characteristics and coolant flow distribution of a NASA-designed air-cooled turbine vane. The vane had chordwise fins which increased the effective heat transfer area in that region by a factor of 3. It was operated in a turbojet engine at turbine inlet gas temperatures to 1644 K (2500° F), coolant inlet temperatures to 700 K (800° F), gas pressures of the order of 31 N/cm^2 (45 psia), and coolant-to-gas flow ratios to 0.187.

The experimental data were used to validate heat transfer correlations for average and local midspan temperatures. A correlation that employs a temperature difference ratio (which considers the effective gas temperature, the cooling-air temperature, and the vane wall temperature) as a function of the ratio of coolant-to-gas flow is the one recommended.

Equations that fit the correlated data were determined. The measured midspan wall temperatures generally differed by no more than ±5 percent from those determined by the correlation equations.

Because the vane had undesirably high leading-edge temperatures, high chordwise thermal gradients, and excessive coolant pressure requirements, it was analytically redesigned. For a turbine inlet total temperature of 1509 K (2257° F), a coolant temperature of 922 K (1200° F), and a coolant-to-gas flow ratio of 0.05, calculations indicated the modified vane would have a maximum leading-edge temperature of 1278 K (1840° F), which was 134 K (241° F) less than that of the original vane. The average midspan temperature for the modified vane was calculated to be 2 K (3.6° F) less than that for the original vane. The difference between the leading-edge maximum temperature and the minimum midchord temperature was 152 K (274° F) for the modified vane compared to 294 K (529° F) for the original vane. The modified vane required substantially less pressure for a given airflow than did the original vane.

INTRODUCTION

The purposes of this report are (1) to present experimental heat transfer data obtained from an air-cooled chordwise-finned turbine vane; (2) to validate a heat transfer correlation and compare measured temperatures with those calculated from experimentally determined correlation equations; (3) to compare measured temperatures with analytically determined temperatures; (4) to present a method of obtaining the coolant flow distribution through a multiexit vane; and (5) to evaluate and improve the design of the chordwise-finned vane.

The NASA Lewis Research Center is engaged in a continuing program to investigate turbine cooling for application to aircraft gas turbine engines. A part of this program calls for the heat transfer investigation of turbine vanes which employ combinations of impingement cooling, film cooling, and convection cooling. Ideally, wall temperatures for these vanes should be determined analytically. However, until adequate analytical prediction methods become available, semiempirical correlations such as those presented in reference 1 are required for predicting vane wall temperatures. Some results of this turbine cooling investigation are presented in references 1 to 5.

Reference 5 presents temperature data from a four-vane cascade for the same chordwise-finned vane configuration of this report. It then compares those data with the equation of the mean line for the data contained herein, which are from a turbojet engine. The main emphasis in reference 5 is on the comparison between data from a cascade with data from an engine, whereas in the present report the emphasis is on the vane configuration itself. Reference 5 considers neither the determination of the coolant flow distribution nor the improvement of the cooling configuration.

The vanes investigated in this report have a span of about 10.2 centimeters (4 in.) and a chord of about 6.4 centimeters (2.5 in.). The vane cooling design incorporates impingement, film, finned and ordinary convection cooling principles. Impingement cooling is applied to the leading-edge region. Film cooling is applied to the external pressure and suction surfaces immediately aft of the leading edge. Internal finned convection cooling employing chordwise passages is used in the midchord region of the pressure and suction surfaces. These chordwise passages increase the effective heat transfer area in this region by a factor of approximately 3. The cooling air from these passages flows through a split trailing-edge, cooling it by convection.

Five test vanes with thermocouples imbedded in the walls were installed adjacent to each other in the stator assembly of a turbojet engine. This engine was modified specifically for the investigation of air-cooled turbine vanes and blades. The cooling characteristics of the vanes were determined over a range of turbine inlet temperatures that varied from 1033 to 1644 K (1400° to 2500° F), for vane inlet coolant temperatures that ranged from 300 to 700 K (80° to 800° F), for ratios of coolant-to-gas flow from 0 to

0.187, and for a small range of gas pressures that were of the order of 31 N/cm^2 (45 psia).

In addition to the heat transfer, two other classes of tests and results are reported. A vane with the cooling configuration just described was investigated in a cold-air flow facility so that calibrations of the coolant flow distribution through the vane could be obtained. Two solid vanes (no internal cooling) having the same external geometry as the cooled vanes were instrumented with pressure taps and were tested in the engine so that an external pressure distribution around the vane periphery could be measured.

Mr. Daniel J. Gauntner assisted in calculating local vane metal temperatures for this research project.

APPARATUS

The vanes that were investigated for their heat transfer characteristics were installed in a turbojet engine that was modified to permit research testing of air-cooled turbine vanes. The engine was installed in a test cell and operated at sea-level conditions. A complete description of engine, test cell, instrumentation systems, and data acquisition systems is given in reference 2. A brief description of the engine and the test facility is provided herein for general information purposes.

Engine

The engine that was modified to make the turbine cooling research engine is a conventional two-spool J75 turbojet engine. Only the high-pressure spool of the basic engine is used. The research engine consists of a seven-stage axial flow compressor, a can-annular combustor, and a single-stage turbine. Provision is made for two separate cooling-air systems in the turbine stator assembly. The coolant temperatures and flow rates of these systems can be adjusted independently of each other.

The complete turbine stator assembly consists of 72 vanes. In the research engine, provision is made for a group of five test vanes to be installed adjacent to each other; these five vanes are supplied cooling air from a laboratory air system that is independent of the system supplying coolant to the remaining 67 vanes in the stator. The remaining vanes in the assembly are workhorse vanes which remain in the stator assembly while research vanes are investigated for their cooling performance. Both the leading edge and midchord regions of this workhorse vane configuration are impingement cooled. It also has a split trailing edge which is film cooled on both the suction and pressure surfaces. A complete description of this vane appears in both references 1 and 5. The re-

search vanes shall be identified as test vanes, and the workhorse vanes shall be identified as slave vanes.

Test Cell

The engine draws the air from the test cell through a preheater, a plenum chamber, a cone-shaped antidebris screen, and a bellmouth ahead of the engine inlet section. The preheater contains an array of 27 combustor cans which are fired with natural gas. The temperature of the vitiated air at the exit of the preheater can be controlled automatically to values ranging from about 353 to 478 K (175° to 400° F).

A test cell data system provides for the acquisition of 260 pressures and 200 temperatures (thermocouples) for research purposes. Turbine-type flowmeters and tachometer transducers are used to produce frequency signals proportional to fluid flow rates and engine speeds. The various types of data are recorded automatically by a central data recording and computer system. A typewriter terminal, which is part of the time-sharing central computer system, is located in the test cell control room. This system permits the central computer to provide computed test results, as well as instrumentation channel checks, to the test facility within minutes of recording. Instrumentation for visual readout in the test cell control room is also provided for facility operational purpose.

Vane Description

The vane of this report was designed to operate at a coolant inlet temperature of 922 K (1200° F) and a coolant-to-gas flow ratio of 0.05 split equally between the impingement holes in the leading edge and the chordwise passages in the afterbody region. The allowable hotspot vane metal temperature is 1278 K (1840° F).

External geometry. - The test vane assembly is shown in figure 1. The vane airfoil has a span of about 10.2 centimeters (4 in.) and a chord of about 6.4 centimeters (2.5 in.). The aerodynamic profile of the test vane airfoil is the same as that of the slave vane. When the vanes are installed in the stator assembly, the hub and tip platforms form the inner and outer end walls, respectively, of the stator gas flow channels. The tip platform is provided with an air inlet tube to permit entrance of the cooling air into the vane.

Cooling configuration. - The vane internal cooling geometry is illustrated in figure 2. The cooling air from the air inlet tube is ducted into a central plenum chamber within the airfoil, as shown in figure 2. From this cavity the cooling air is distributed

to a row of impingement holes in the forward portion of the plenum and to a series of chordwise passages with their entrances in the midchord region of the plenum.

The row of impingement holes is formed by 46 holes spaced 0.203 centimeter (0.080 in.) apart, center to center, and having a diameter of 0.127 centimeter (0.050 in.). The spacing between the row of impingement holes and the inside leading-edge surface can be expressed as 5.24 hole diameters or 10.7 equivalent slot widths. The equivalent slot width is defined as the area of one impingement hole divided by the center-to-center spacing between two adjacent holes.

After the coolant impinges upon the inside surface at the leading edge, it flows rearward in a chordwise direction along the internal suction and pressure surfaces and exits through film cooling holes located about 1.78 centimeters (0.7 in.) downstream of the leading-edge stagnation point. The suction-surface film cooling holes consist of 58 holes having centers equally spaced 0.157 centimeter (0.062 in.) apart and having a diameter of 0.064 centimeter (0.025 in.). These holes are angled at about 28° with respect to an imaginary line tangent to the suction surface at the exit region. The pressure-surface film cooling holes consist of two rows of 0.071-centimeter (0.028-in.) diameter holes equally spaced (center to center) 0.157 centimeter (0.062 in.) apart. There are 58 holes in the row closest to the leading edge and 59 holes in the aft row. The chordwise centerlines of the aft row of holes are offset with respect to the chordwise centerlines of the forward row of holes by a radial distance of 0.079 centimeter (0.031 in.). Both rows of holes are inclined at an angle of about 40° to an imaginary line tangent to the pressure surface at the location of the holes.

The remaining cooling air in the plenum chamber (other than that air flowing through impingement holes) enters a series of chordwise passages adjacent to the suction and pressure surfaces. The entrance to these passages is in a spanwise plane about 3.05 centimeters (1.2 in.) from the leading-edge stagnation point. The chordwise passages are nominally 0.076 centimeter (0.030 in.) square. The fins are nominally 0.025 centimeter (0.010 in.) thick. There are a total of 91 passages adjacent to both the suction and pressure surfaces. The passages extend in a chordwise direction to a spanwise plane about 1.45 centimeters (0.57 in.) from the extreme trailing edge; in this plane the flow passages adjacent to the suction surface join with the flow passages adjacent to the pressure surface to form a single flow passage. About 0.64 centimeter (.25 in.) from the trailing edge, the passage divides into six equally spaced flow channels that are about 1.384 centimeters (0.545 in.) high and 0.076 centimeter (0.030 in.) wide. The coolant flows through these channels and is expelled into the gas stream from the extreme trailing edge of the vane. The channels are formed by lands that are 0.254 centimeter (0.10 in.) high, have a length of about 0.64 centimeter (0.25 in.) and are spaced about 1.385 centimeters (0.545 in.) apart.

Fabrication. - The fabrication approach that was used involved the fabrication of

several subassemblies that were subsequently brazed or welded together to form the complete vane assembly. Solid one-piece castings having the approximate external geometry of the vane airfoil and the integral hub and tip platforms were made from Udimet 700 material. These castings were then electrical discharge machined to obtain the final internal and external contours. Figure 3 shows views of the inside surface of the completely machined airfoil sections for the suction and pressure sides of the vane. Contoured cover sheets of 0.013-centimeter (0.005-in.) thick L605 material were furnace brazed to the edges of the chordwise fins. These cover sheets formed the fourth surface for the square-cross-section coolant passages in the aft portion of the midchord region of the airfoil; they also formed a portion of the wall of the central plenum chamber (fig. 2). Figure 4 shows the coolant side of the airfoil suction and pressure surfaces with the fin cover sheets brazed in place. Figure 4 also shows the hole partition pieces brazed in place. These pieces were brazed to the partition lands and the vertical lands shown in figure 3. The partition was made in two pieces with one part being furnace brazed to the suction-side assembly, and the other to the pressure-side assembly. Each piece of the orifice partition was brazed to five chordwise lands and to a single vertical land machined in the coolant-side surface near the leading-edge region of the respective suction- and pressure-surface subassembly (fig. 3). The piece of the partition brazed to the pressure-surface subassembly contained the impingement holes. The thin contoured cover sheets and the hole partition pieces were brazed to their respective subassemblies in a single brazing operation.

Next, the two major subassemblies were prepared for bonding together to form a single vane assembly. The suction- and pressure-surface subassemblies were then placed in a fixture, and the subassemblies were electron beam welded together at the mating faces of the airfoil and at the hub and tip platforms. The mating face at the leading edge of the airfoil extended from the hub to the tip at the extreme leading edge (stagnation point region). In the airfoil trailing edge the subassemblies were electron beam welded where the trailing-edge lands on the suction-surface subassembly (figs. 3(a) and 4(a)) mated with the coolant-side surface in the pressure-side subassembly. The assembly was also electron beam welded along the mating faces on the hub and tip platforms. After the electron beam welding was completed, the vane assembly was placed in a furnace and the hole partition pieces and the fin cover sheets were brazed together.

The final fabrication steps were to attach the tip platform cover plate and the cooling-air inlet pipe to the tip platform and to final machine grind the hub and tip platforms to the desired contours. A completed vane assembly is shown in figure 1.

Installation in engine. - The five test vanes were installed adjacent to each other in the engine as indicated in the schematic diagram of figure 5. The test vanes were located at the bottom portion of the stator assembly. The test vanes were numbered from

1 to 5 according to their position in the vane assembly as indicated in figure 5; this numerical identification of the test vanes is used throughout the report.

Calibration Vane Description

In addition to the test vanes described in the preceding section, two calibration vanes were used to obtain the gas-side static pressure distribution around the airfoil. Solid noncooled airfoil sections were selected for the pressure distribution calibration tests so that a relatively large number of pressure taps and the associated tubing for pressure leads could be installed in the airfoils without seriously weakening the airfoil structure. The use of noncooled vanes, however, restricted the maximum average turbine inlet temperature of the engine to about 1255 K (1800° F) when the calibration vanes were installed in the stator assembly.

INSTRUMENTATION

Engine

The research engine is instrumented extensively to provide information on the general operating conditions of the engine and also to provide detailed information relative to the environmental conditions in the turbine test section. The instrumentation consists primarily of temperature (thermocouple) and pressure measurements to determine airflow, combustion gas flow, and state conditions in various portions of the engine such as the compressor inlet, the compressor discharge, the turbine inlet, and the turbine discharge. At the turbine inlet station, eight remotely actuated water-cooled temperature probes are used to determine the composite turbine inlet temperature profile. One of these probes is located behind each combustor. The probe positions are at eight different circumferential distances from the radial centerlines of the combustors. Each probe is traversed in a radial direction and is programmed to stop automatically at nine equally spaced locations. The eight circumferential probe positions and nine radial stops of each probe provide 72 different points of temperature measurement for the composite profile. The details of the instrumentation in the combustion air, combustion gas, and cooling-air systems are given in reference 2.

Test Vane

Thermocouples. - The five test vanes were instrumented with a total of 25 Chromel-

Alumel thermocouples imbedded in the walls of the airfoils. The thermocouple locations and location numbers are shown in figure 6. Note that the leading-edge location numbers 7 and 20 have been duplicated. The midspan plane of the airfoil is considered the "test section," so a majority of the thermocouples (14) were placed at the midspan. Four thermocouples were placed at the hub plane (1.63 cm (0.64 in.) from the hub platform) and seven thermocouples were located at the tip plane (1.63 cm (0.64 in.) from the tip platform). Because of structural considerations, the maximum number of thermocouples installed on any given test-vane airfoil was seven. It was necessary, therefore, to place the 14 midspan thermocouples on more than one vane. Three midspan thermocouples were placed on the suction surface of vane 2, seven on the pressure and suction surfaces of vane 3, and four on the pressure surface of vane 4.

The cooling-air temperature at the inlet to individual vanes is determined from a single Chromel-Alumel thermocouple installed downstream of the entrance to the inlet tube. Vanes 2, 3, and 4 were equipped with cooling-air inlet thermocouples.

Pressures. - A single wall static pressure is used to indicate the cooling-air pressure at the inlet to an individual vane. The wall static tap is located in a straight section of a cooling-air inlet pipe that is an extension of the cooling-air inlet tube. The tap is located upstream of the tip platform.

Calibration Vanes

The two solid noncooled calibration vanes were instrumented with a total of 30 static pressure taps to measure the vane surface static pressures. Table I summarizes the locations of the pressure taps on the two calibration vanes. The procedure for installing the pressure taps and the tubing leads was the same as that described in reference 3.

The gas-stream static pressure at the exit of the vane row was obtained from a single static pressure tap located in the gas-side wall of the hub and tip platforms of vane 2. The taps were located in the platforms so that when the vanes were assembled in the engine, the taps were midway (in a transverse direction) between the suction surface of vane 2 and the pressure surface of vane 3 in a plane about 0.48 centimeter (0.19 in.) downstream of the extreme trailing edges of the vane airfoils.

TEST PROCEDURE

Calibration Tests

Prior to investigating the test vanes for their coolant flow distribution and heat

transfer characteristics, a determination of the static pressure distribution around a typical vane airfoil was made. For the pressure distribution calibration, the two calibration vanes discussed previously were installed in the stator assembly. The calibration vane with the static taps in the suction surface was installed in vane position 2 (positions defined in fig. 5); the vane with the pressure-surface taps was installed in position 3. Solid noncooled, noninstrumented vanes having the same geometry as the calibration vanes were installed in positions 1, 4, and 5. All other vanes in the stator assembly were slave vanes. Static pressure data were obtained at increments of about 100 rpm over the range of engine speeds from 6740 to 8020 rpm. The range of engine operating conditions covered during the pressure distribution calibrations are given in the following table:

Engine condition	Minimum	Maximum
Engine speed, rpm	6740	8020
Average turbine inlet temperature, K (^{o}F)	765 (917)	1276 (1838)
Stator inlet total gas flow, kg/sec (lb/sec)	20.5 (45.2)	35.0 (77.2)

Coolant Flow Distribution Tests

The relation between the distribution of the cooling air within the vane and the ratio of the coolant inlet pressure to coolant exit pressure was determined from "bench-type" tests made in a cold-air flow facility. Flow collectors similar to those shown in figure 3 of reference 4 were attached to each of the three vane exits. The flow quantities through the vane exits (the pressure-surface film cooling holes, the suction-surface film cooling holes, and the trailing-edge holes) could then be individually measured. Data were obtained over a range of total coolant flow rates through the vane. The flow rate was controlled by adjusting the cooling-air static pressure at the vane inlet $P_{c,i}$ while maintaining a given relation among the three vane exit static pressures P_o. (All symbols are defined in the appendix.) This relation was established by the tests on the solid calibration vanes.

Heat Transfer Tests

For the heat transfer tests the five thermocoupled test vanes were installed in the

engine stator assembly in the positions indicated in figure 5. The engine was operated over a range of turbine inlet temperatures from about 1033 to 1644 K (1400° to 2500° F). The engine speed ranged from about 6800 to 8700 rpm. Most of the tests were made with the cooling-air temperature at the vane inlet at a value of about 300 K (80° F). Two series of runs, however, were made at nominal cooling-air inlet temperatures of 478 and 700 K (400° and 800° F). Most of the tests were made at a constant compressor inlet air temperature of about 450 K (350° F), although two series were made with a compressor inlet temperature of 300 K (80° F). The compressor pressure ratio had a value of approximately 3 with the engine inlet exposed to atmosphere. Vane metal temperature data and vane coolant flow data were taken over the complete range of operating conditions in order to obtain the heat transfer characteristics of the test vanes. Generally, the test vane data were obtained with constant amounts of cooling air being supplied to the slave vanes during a given series of runs. The values of the major engine operating parameters associated with each series of runs are given in table II.

The engine operating procedure is to start a given series of tests with a relatively large coolant flow to the test vanes. Large amounts of coolant are also supplied to the slave vanes to overcool the slave hardware throughout the test program. The engine speed is adjusted to obtain the desired average turbine inlet temperature; and when equilibrium conditions are reached, the data for the first run of the series are taken. A series of tests is defined herein as a group of runs made at constant turbine inlet temperature and constant cooling-air temperature; a change of coolant flow rate is the primary variable from run to run. For each successive run in a series of tests, the coolant flow to the test vanes is reduced relative to the flow rate for the previous run.

The test vane coolant flows are reduced stepwise for each series of runs until a maximum vane airfoil metal temperature of about 1255 K (1800° F) is reached; this is considered the maximum safe operating temperature for the vane configuration. After the minimum coolant flow condition is reached, a few additional runs at increased coolant flow are made to serve as checkpoints for the data taken previously. This general procedure is usually repeated for each series of runs. The test vane coolant flow ratios ranged from about 0 to 0.187 (table II). In order to maintain the nominal average turbine inlet temperature constant, the engine speed for some series of tests could vary as much as 200 to 500 rpm.

ANALYSIS METHODS

Evaluation of External and Internal Vane Parameters

The horizontal finned vane of this report incorporates impingement, film, and con-

vection cooling. In order to calculate metal temperatures for this vane, it is necessary to know certain conditions which exist at the interface of the vane surface with the combustion gas. These interface conditions are discussed in detail in reference 1. Only a brief mention of each is made here.

Pressure distribution. - The pressure distribution around the vane profile can be obtained either from experimental measurements or from a calculation method. Experimentally measured pressure distributions around a solid vane of the same airfoil shape as the chordwise-finned vane were obtained and are presented later. Calculation procedures for estimating the external pressure distribution around an airfoil are presented in references 6 and 7. The experimental values are used for determining the local coolant flow rates which are used in correlating the data.

Convection gas-to-metal heat transfer coefficients. - For the vane leading-edge region, the equation for flow over a cylinder (ref. 8, p. 373) is used. It is

$$Nu_D = 1.44\, Re_D^{0.5} Pr^{0.4} \left(1 - \left|\frac{\theta}{90}\right|^3\right) \tag{1}$$

where θ is the angle measured from the stagnation point and is limited to $-80^\circ < \theta < 80^\circ$.

Reference 5 presents predicted temperatures for a vane tested in both a high-temperature cascade and in the research engine of this experimental study. The previous equation was found to be adequate for predicting cascade leading-edge vane temperatures, while an additional factor of 1.35 was necessary for predicting engine leading-edge vane temperatures. This factor was attributed to the effects of turbulence and radiation and to the uncertainty in the gas temperature profile. It was determined experimentally from the following equation:

$$\frac{h_{g,\,engine}}{h_{g,\,cascade}} = \frac{\left(\frac{1-\varphi}{\varphi}\right)_{engine}}{\left(\frac{1-\varphi}{\varphi}\right)_{cascade}} = 1.35 \tag{2}$$

In equation (2), $(1 - \varphi)/\varphi$ equals $(T_w - T_c)/(T_{ge} - T_w)$, the values of T_{ge}, T_c and $\dot{w}_c/\dot{w}_g$ for the engine equal those of the cascade, and T_w is the corresponding leading-edge hotspot temperature from the engine and cascade.

For the other convection-cooled parts of the vane, the turbulent flow flat-plate equation (ref. 9, p. 198) is used. It is

$$Nu_x = 0.0296\, Re_x^{0.8} Pr^{1/3} \tag{3}$$

The gas properties for equations (1) and (3) are based on the reference temperature (ref. 10, p. 270)

$$T_{ref} = 0.28\ T_{st} + 0.5\ T_w + 0.22\ T_{ge} \tag{4}$$

Effective gas temperature. - Because the effective gas temperature T_{ge} is assumed equal to the adiabatic wall temperature, the T_{ge} can be expressed in terms of the recovery factor Λ.

$$T_{ge} = T' - \frac{(1 - \Lambda)v_y^2}{2g_c c_p} \tag{5}$$

where T' is the total temperature, v_y is the local velocity, and Λ is the recovery factor. For turbulent flow, $\Lambda = Pr^{1/3}$. For Mach numbers less than 0.3, which are typical of a vane leading edge, the effective gas temperature is at least 99.5 percent of the total temperature. Therefore, the values of recovery factor at these low Mach numbers are of no practical use.

Film cooling effectiveness. - The film effectiveness is often expressed in the form

$$\eta_f = C_2 Re_{c,s}^{p} \left(\frac{x}{Ms}\right)^{-q} \tag{6}$$

The slot width s in equation (6) is obtained by equating the total area of the film cooling holes on a given surface to the area of an equivalent slot running the span of the vane. For present application, the following equations are taken from reference 11 and are the results of tests on models:

$$\eta_f = -0.00001\left(\frac{x}{Ms}\right)^{1.952} + 0.5 \tag{7}$$

for the suction surface and

$$\eta_f = -0.026\left(\frac{x}{Ms}\right)^{0.498} + 0.5 \tag{8}$$

for the pressure surface.

These values of η_f were then used in

$$\eta_f = \frac{T_{ge} - T_{aw}}{T_{ge} - T_{c,s}} \tag{9}$$

to obtain the adiabatic wall temperature T_{aw}. This temperature is used in place of the effective gas temperature for determining the heat flux to a film-cooled surface.

Convection metal-to-coolant heat transfer coefficient. - For the impingement-cooled leading-edge region, a local heat transfer correlation is obtained by combining correlations from references 12 and 13. The ratio of local to average heat transfer coefficients is obtained from reference 12. To obtain this ratio, an expression for the local Stanton number is divided by an expression for the average Stanton number, with both expressions being evaluated at an optimum spacing between the jet hole and the heat transfer surface. The resulting relation expressed in terms of Nusselt numbers appears below

$$\frac{Nu(x)}{\overline{Nu}} = 0.475\left(\frac{x}{l}\right)^{-0.475} \tag{10}$$

where x is measured from the stagnation point and l is $\pi D/4$. The average Nusselt number is obtained from reference 13 and appears here in a different form:

$$\overline{Nu_n} = 0.36\, Re_n^{0.62}\left(\frac{D_n}{2l}\right)^{0.38} \tag{11}$$

The product of these two expressions yields an expression for the local heat transfer coefficient around the inner surface of the leading edge.

For all other regions of the vane, the vane-to-coolant heat transfer coefficients are obtained from the following correlation from reference 14:

$$Nu_{D_h} = 0.0205\, Re_{D_h}^{0.8} Pr^{0.333} \tag{12}$$

When applied to portions of the vane which have finned surfaces, the constant in the previous equation is increased by the fin effectiveness equation from reference 15:

$$\frac{h_{fin}}{h_i} = \frac{2\tanh \varphi_{fin} L_{fin}}{\varphi_{fin}} + m_{fin} \tag{13}$$

where $\varphi_{fin} = (2h_i/k_w\tau_{fin})^{1/2}$, m_{fin} is the surface-to-surface fin spacing, τ_{fin} is the fin thickness, and L_{fin} is the effective fin width.

Experimental Vane Metal Temperature Correlations

Correlation equations. - A method for curve fitting the experimental heat transfer data for a surface cooled by convection is presented in reference 1. The resulting correlation equation is

$$Y = \frac{K\left(\frac{\dot{w}}{\mu}\right)_g^n}{\left(\frac{\dot{w}}{\mu}\right)_c^m} \tag{14}$$

where the exponents m and n and the constant K are curve-fit constants which are discussed later and

$$Y = \frac{1 - \varphi}{\varphi} \frac{Pr_c^{1/3} k_c}{Pr_g^{1/3} k_g} \tag{15}$$

and

$$\varphi = \frac{T_{ge} - T_w}{T_{ge} - T_c} \tag{16}$$

Some surfaces have convection cooling augmented by film cooling at selected locations. Reference 1 also considers this case and arrives at a data correlation equation

$$\frac{Y}{\left(\frac{\dot{w}}{\mu}\right)_g^n \Big/ \left(\frac{\dot{w}}{\mu}\right)_c^m} = K\left[1 - \frac{\eta_f}{\varphi}\left(\frac{T_{ge} - T_{c,s}}{T_{ge} - T_c}\right)\right] \tag{17}$$

When $\eta_f = 0$, equation (17) reduces to equation (14).

A correlation useful in comparing the cooling effectivenesses of vanes with different internal cooling configurations was derived in reference 16. It is

$$\overline{\varphi} = \frac{1}{\frac{F}{\eta_t} + 1} \tag{18}$$

where η_t is the thermal effectiveness given by

$$\eta_t = \frac{\overline{T}_{c,o} - T_{c,i}}{\overline{T}_w - T_{c,i}} \tag{19}$$

and F is defined as

$$F = \frac{\overline{h}_g S_g}{\dot{w}_c c_{p,c}} \tag{20}$$

Simplification of correlations. - If property values are deleted from equations (14) and (15), and if the exponents are assumed to be equal, the following correlation results:

$$\frac{1 - \varphi}{\varphi} = A\left(\frac{\dot{w}_c}{\dot{w}_g}\right)^{-B} \tag{21}$$

Although the data in this report are actually curve fit to equation (21), they are presented as φ against $\dot{w}_c/\dot{w}_g$ because of convention.

If the data scatter about the latter correlation is acceptable, there is no need to consider the other correlation. Either of these correlations can be applied to average or local data.

Application to vane. - Application of the preceding correlations is limited to the midspan section of the vane where most of the thermocouples were installed. Initially, the correlations are applied to average values. For this purpose, an average value is determined by use of the inlet coolant temperature for the average coolant temperature, the turbine inlet total gas temperature for the average effective temperature, and the average wall temperature. In this report the turbine inlet total gas temperature T_{Ti} is the circumferential average of the eight turbine inlet probes at the three middle radial positions.

Use of the circumferential average gas temperature may be somewhat misleading. Since in the engine the local effective gas temperature varies from vane to vane, the driving temperature difference likewise varies as does the temperature at identical points on adjacent vanes. For low gas temperatures an adiabatic wall temperature distribution can be determined by eliminating all coolant flow; the resultant vane metal temperature distribution can then be equated to the effective gas temperature distribution. However, the level of the gas temperatures of this investigation precluded such a

determination of local effective gas temperature. Therefore, the circumferentially averaged gas temperature was used for correlating the data.

As noted in reference 1, T_{Ti} at the midspan has essentially the same value as the integrated average of the local midspan values of T_{ge}, and $\overline{T}_w$ is the integrated average of the local midspan values of T_w. The coolant flow per vane and the gas flow per vane channel are also used. Finally, property values are based on $T_{c,i}$ and T_{Ti} for the coolant and gas, respectively.

In applying the correlations to a local midspan position, φ is determined as before by again using T_{Ti} and $T_{c,i}$, but this time the local value of T_w is used. Again, property values are based on $T_{c,i}$ and T_{Ti} for the coolant and gas, respectively. One set of calculations are made by using the coolant flow per vane. A second set is made by using the coolant flow to a particular exit of the vane such as the trailing edge.

Determination of exponents in correlations. - The exponents occuring in the correlation equations previously discussed are determined as follows: For application to average conditions, a plot of $\ln(\overline{Y})$ against $\ln(\dot{w}/\mu)_c$, with $(\dot{w}/\mu)_g$ as the parameter, yields lines whose slopes are the negative of the exponent m from equation (14). A crossplot of this figure yields a plot of $\ln(\overline{Y})$ against $\ln(\dot{w}/\mu)_g$ whose slope is n from equation (14).

When local conditions are considered, exponents m and n are found for each local position, in a similar manner to that just described, except that the local values of Y are now used as the ordinates. It should be noted that the local values of m and n are different at each local position and are also different from those obtained whan averages are considered.

Predicted Metal Temperature

The flow distribution of the coolant as it passes through the vane internal cooling passages is required to predict local vane temperatures. A one-dimensional compressible flow model of the internal cooling configuration is used. Experimentally measured pressures and flow distributions made in separate cold-flow tests of the chordwise-finned vane are used. These tests are discussed in the section Coolant Flow Distribution Tests. By use of these data, flow characteristics such as inlet and exit losses and friction pressure drops can be determined. These flow characteristics are used to establish the required flow coefficients in the one-dimensional flow model which would result in flow distributions which match the measured flow distributions for the cases considered.

With the flow coefficients now available, the flow distribution through the vane can be determined. By use of the available measured vane external pressures, the measured total coolant flow rate, and the measured inlet coolant temperature, the flow distribution

through the vane can be determined by iterating on the inlet pressure until the calculated total flow converges to the measured total flow.

To predict vane temperatures, other quantities have to be known. From the discussions already presented, the effective gas temperature distribution, the gas-to-vane heat transfer coefficients, and the vane-to-coolant heat transfer coefficients can be estimated.

For the heat transfer calculations, a nodal network for the vane wall was established. Assumed initial vane metal temperatures must be used to evaluate the gas properties based on the reference temperature in the gas-to-vane heat transfer coefficients. Then the combined flow and heat transfer programs are used, with the known flow characteristics as described previously, and vane temperatures are determined. Iteration between flow and heat transfer is required until the calculated vane temperatures converge and the calculated total flow matches the measured total flow.

Comparison of Measured and Calculated Flow Distributions

The combined flow and heat transfer calculation procedure yields values of the coolant flow through the individual exits of the vane. These values can be compared with experimental values of the flow through the same vane exits. The experimental values will be obtained from the measured coolant inlet and turbine inlet gas pressures from the engine tests and from correlations of the cold-flow data obtained from the separate cold-flow tests.

RESULTS AND DISCUSSION

Structural Damage Due to Heat Transfer Testing

The test program as shown in table II started with a 1033 K (1400° F) gas temperature test series and ended with a 1644 K (2500° F) test series after which the entire test program was repeated. The cooling performance at the vane leading edge started to decrease around the time of the first 1644 K (2500° F) test series and gradually became poorer over the entire repeat portion of the test program. To investigate the cause of this decrease in cooling performance, the interior geometry of the vanes were viewed through a boroscope after the completion of the test program. This visual inspection revealed that the orifice partitions (shown in fig. 3) in all five vanes separated from the vertical lands on both the suction and pressure surfaces. These separations allowed the cooling air to pass from the central plenum chamber directly to the film cooling holes without first cooling the leading edge by impingement.

Other structural failures also occurred. Two of the five vanes had spanwise separations at the leading edge along the seam where the two half-vane subassemblies had been bonded together. These separations covered over 50 percent of the vane span. A chordwise crack also occurred on these two vanes at the midspan. These cracks extended from the leading-edge spanwise separations to one of the film cooling holes on the pressure surface.

The interior inspection of the vane also revealed that the contoured sheets, which had been furnace brazed to the edge of the chordwise fins to form the fourth surface of the coolant passages, had slight tears and had become slightly detached from the fins in the vicinity of the tears.

Because no absolute method is available for determining when these failures occurred, only those data are presented which were recorded before the cooling performance at the leading edge started to decrease.

External Static Pressure Distribution

It was stated previously that static pressure measurements were made around the periphery of two solid vanes of the same external profile as the chordwise-finned vanes. Data are presented for three midchannel, exit Mach numbers at the midspan. Figure 7 shows these distributions around the vane; the static-pressure-to-inlet-total-pressure ratio is plotted as a function of the dimensionless distance x/L along the surface from the stagnation point. The distributions are typical pressure distributions around a vane; the pressure ratio generally decreases slightly as the Mach number is increased from 0.74 to 0.92. These experimental values are used in determining the local coolant flow rates through the vane as discussed in the section Coolant Flow Distribution Tests.

An analytical pressure distribution around the vane was also obtained by the method discussed in reference 7; it was used in the prediction of heat transfer coefficients for the analytical temperature calculations. This pressure distribution agreed very favorably with the experimentally determined distributions and, hence, is not shown on figure 7.

Gas Temperature Profile

Corresponding positions of each of the eight probes are averaged to obtain a turbine inlet temperature profile. A typical profile, shown in figure 8, displays a rather drastic change near the vane tip. This may be due to combustor diluent air and possibly some slight (about 0.305 cm (0.120 in.)) radial mislocation of the temperature probes.

In any event the effective gas temperatures employed herein are those from the three probe positions in the midspan position of the duct where the gas temperature is nearly constant. These three positions are averaged over the eight probes to obtain an average midspan turbine inlet temperature. These average midspan turbine inlet temperatures, as well as the measured vane wall temperatures, are presented in table II of this report.

Coolant Flow Distribution Tests

The results of the cold-flow distribution tests are presented in figure 9, which shows the distribution of the cooling air within the vane as a function of the coolant pressure at the inlet of the vane to the gas pressure at the inlet of the turbine. This type of plot results from the measurement of the flow rates in flow collectors surrounding the three flow-exiting locations, measurement of the inlet coolant flow temperature and static pressure, and measurement of the static pressures in the flow collectors. These flow collector pressures, established by using figure 7, were 0.60, 0.725, and 0.88 of the expected turbine inlet total pressure at an x/L of 1.0 for the trailing edge, and x/L of 0.31 for the suction-surface film cooling holes, and an x/L of 0.33 for the pressure-surface film cooling holes, respectively.

In the engine calibration tests, mentioned in the section TEST PROCEDURE, the gas-side static pressure distribution around the vane periphery is measured. In the engine heat transfer tests, the inlet temperature and static pressure of the flow are measured. Hence, for each of the three flow-exit positions, a value of the abscissa $P_{c,i}/P_{Ti}$ is known. From the cold-flow data plot of figure 9, a value of the ordinate $\dot{w}_{c,x}\sqrt{T_{c,i}}/P_{c,i}$ can be read corresponding to the appropriate value of $P_{c,i}/P_{Ti}$. Finally, the three desired values of $\dot{w}_{c,x}$ can be calculated since $T_{c,i}$ and $P_{c,i}$ are measured.

The sum of the three calculated values of $\dot{w}_{c,x}$ will not equal the measured total flow because the calibration curves of figure 9 were obtained for a constant cooling-air temperature. In actual engine operation, the cooling air inside the vane and at the discharge points was heated to a higher temperature than the measured inlet temperature $T_{c,i}$. Each of the three local values of $\dot{w}_{c,x}$ is, therefore, adjusted by multiplying by the ratio of the total measured flow to the total calculated flow. In this way, the sum of the calculated local flows is forced to equal the total measured flow. Some inaccuracy exists since the coolant air will not necessarily be heated the same amount at the three discharge points.

With the data presented as in figure 9, the expected range of coolant flows can be quickly determined. Above a pressure ratio of about 1.05, the engine compressor can-

not supply the cooling air to the inlet of the vane at a sufficiently high pressure. Below 0.88, the hot gas will be drawn into the vane through the pressure-surface film cooling holes.

The fraction of the total coolant which flows through each of the three coolant exit passages can be obtained from figure 9. To accomplish this, each of the three values of the ordinate, for a given pressure ratio, is divided by the sum of the three.

These calculations were performed over the entire range of the pressure ratio shown in figure 9. The flow rate characteristics of the vane can be displayed as in figure 10. Only the pressure ratio range from 0.88 to 1.05 is practical for engine application; however, an extended range up to 1.8 appears in figure 10. This extended pressure ratio range is included so as to cover most of the pressure ratios encountered in the heat transfer testing.

Figure 10 shows that the percent of flow through the suction-side film cooling holes remained approximately constant for a pressure ratio greater than 0.88 but less than 1.05. Therefore, as the pressure ratio decreases, the coolant-to-gas flow ratio decreases; and so the suction-side temperatures near the film cooling holes should increase. The percent of flow through the pressure-side film cooling holes decreases very rapidly with decreasing pressure ratio within this range. Therefore, the temperatures on the pressure surface near the film cooling holes should rise faster relative to the suction surface for the same decreasing gas-to-coolant flow ratio. The percent of flow through the split trailing edge increases rapidly with decreasing pressure ratio; and so the trailing-edge temperatures should rise at a lower rate relative to the rest of the vane for the same decreasing coolant-to-gas flow ratio.

Three other local flow rates are of interest and can be obtained from the three flow rates already established. The flow rate which is used to impingement cool the leading edge can be obtained by addition of the two flow rates through the suction- and pressure-surface film cooling holes.

The two flow rates associated with the chordwise passages of the midchord suction and pressure surfaces can be approximated from the trailing-edge flow rate and the lengths of the two flow passages. Since the two flows start and finish in common plenums, the pressure drops associated with each of the two flows must be equal. The only difference between the geometry of the finned passages on either side is that the suction-surface passages are slightly longer than the pressure-surface passages. In the cold-flow test work the entire pressure drop has to be due to entrance and exit losses and friction. Since the frictional pressure drop is proportional to the product of the length of the flow path and the square of the flow rate and since the pressure drop on either surface must be equal, the ratio of these two flow rates must be approximately equal to the ratio of the reciprocal of the square roots of the passage lengths. With this relation and the trailing-edge flow rate, the two midchord flow rates can be approximated.

Although it is true that a momentum pressure drop is present during heat transfer testing, it is small relative to the friction pressure drop.

Figures 9 and 10 were derived entirely from cold-flow data and are adequate for determining the flow distribution for an actual engine heat transfer test point since the coolant-inlet-to-turbine-inlet pressure ratio is known. However, these figures are inadequate for determining the flow distribution for some hypothetical test point because the pressure ratio which corresponds to the required coolant-to-gas flow ratio is unknown. Therefore, some actual engine calibration flow data relating coolant-to-gas flow ratio with pressure ratio are necessary if hypothetical operating conditions are to be evaluated.

Figure 11 presents coolant-to-gas flow ratio as a function of pressure ratio for a gas temperature of 1366 K (2000° F) and coolant inlet temperatures of 296, 475, and 689 K (73°, 395°, and 780° F). This figure shows the pressure ratio which is required for a given coolant-to-gas flow ratio and a given coolant inlet temperature.

A crossplot of figure 11, presenting pressure ratio required for a 0.05 coolant-to-gas flow ratio as a function of coolant inlet temperature, is shown in figure 12. From this figure, for example, it can be seen that a 922 K (1200° F) coolant temperature will require a pressure ratio of 1.11.

Therefore, figures 10 and 11, along with a specified coolant-to-gas flow ratio and coolant inlet temperature, determine the flow distribution. It is important to note that the flow distribution through a multiexit vane is a function of the coolant temperature.

Experimental Vane Wall Temperature Distributions

Figure 13(a) presents three chordwise experimental temperature distributions at the vane midspan for a turbine inlet temperature of 1478 K (2200° F), a coolant inlet temperature of 300 K (80° F), and ratios of coolant-to-gas flows of 0.053, 0.070, and 0.109. The three distributions, formed by superimposing the temperatures from individual vanes, exhibit the same general characteristics. Each has a very high temperature at the leading edge and about a 500 K (900° F) lower temperature in the finned midchord region.

The resulting chordwise temperature gradient is probably not as severe as it appears. The composite temperature distribution which is obtained from three test vanes is not necessarily real since the effective gas temperature varies from vane to vane as a result of the varying circumferential turbine inlet temperatures. Indications of the circumferential temperature gradient were obtained at low gas temperatures by eliminating all coolant flow to the vanes. These tests show that the maximum effective gas temperature occurs on the same vane as does the vane wall hotspot and the minimum

effective gas temperature occurs on the same vane as does the vane wall minimum temperature.

The high leading-edge temperatures are also due to both the inefficient placement of the impingement holes relative to the inner surface of the leading edge and the ineffective split of the cooling air between the leading edge and the midchord passages. As can be seen from figure 11, a coolant-to-gas flow ratio of 0.053 at ambient temperature will require a coolant-inlet-to-turbine-inlet pressure ratio of 0.98. By using this pressure ratio and figure 10, it can be shown that only 35 percent of the cooling air flows out through the impingement nozzles (16 percent to the pressure surface and 19 percent to the suction surface).

As the flow ratio (and consequently the pressure ratio) increases from 0.053, a greater percentage of the coolant flow exits through the film cooling holes on the pressure surface (fig. 10). Evidence of this change in flow distribution can be seen on figure 13(a). Thermocouples located near the film cooling holes on the pressure surface ($x/L = 0.33$) exhibit a greater drop in temperature relative to those on the rest of the vane. Increasing the coolant-to-gas flow ratio from 0.053 to 0.109 requires an increase in the coolant-inlet-to-turbine-inlet pressure ratio from 0.98 to 1.285 (fig. 11). As can be seen from figure 10, the coolant flow through the pressure-surface film cooling holes increases from 16 percent of 0.053 (0.00848) to 29 percent of 0.109 (0.0316). While the total flow to the vane increases by a factor of 0.109/0.053, or 2.06, the flow through the pressure-surface film cooling holes increases by a factor of 0.0316/0.00848 or 3.73. Corresponding flows through both the suction-surface film cooling holes and the split trailing-edge slots are increased by factors of only 1.77 and 1.76, respectively. Because of this great increase in flow out of the pressure-surface film cooling holes relative to the other two vane exits, the metal temperature in this area undergoes the greatest decrease.

Figure 13(b) shows the chordwise variation in the vane midspan metal temperatures for both varying gas temperature and varying coolant temperature for a fixed ratio of coolant-to-gas flow. The curves containing the circular and square symbols are for a gas temperature of 1366 K (2000° F) and coolant temperatures of 300 K (80° F) and 478 K (400° F), respectively; the coolant-to-gas flow ratio is 0.08. The curves show the same general trends as shown in figure 13(a). Increasing the coolant temperature from 300 to 478 K (80° to 400° F), while maintaining the coolant-to-gas flow ratio at 0.08, requires an increase in the coolant-inlet-to-turbine-inlet pressure ratio from 1.12 to 1.22 (fig. 11). The coolant flow through the pressure-surface film cooling slot increases from 24.7 to 27.7 percent (fig. 10). As before, the difference between the corresponding local temperatures near the pressure-surface film cooling holes is greater than the average temperature difference. The curves containing the circular and diamond-shaped symbols have the same coolant temperature of 300 K (80° F) but gas

temperatures of 1366 and 1561 K (2000° and 2350° F), respectively. From figure 13(b) the film cooling on the pressure surface appears to be much more effective for the high-gas-temperature test point.

Correlations of Experimental Temperature Data

Average correlations based on total flow. - The average correlations based on total flow are as follows:

$\overline{Y}$ correlations: The average heat transfer parameter $\overline{Y}$ has been shown to be a function of the coolant flow parameter $(\dot{w}/\mu)_c$. This dependence is shown by experimental data in figure 14. Since the data in this figure are for a fixed geometry, similar ranges of $(\dot{w}/\mu)_c$ indicate similar ranges of the Reynolds number. Therefore, all the sets of data in figure 14 should be from approximately the same flow regime and so should have the same slope. Because of this, parallel lines are drawn through each set of data in the figure. The magnitude of the resulting slope is 0.66, which represents the value of m in equation (14).

Figure 15, which is a crossplot of figure 14, shows the dependence of the average heat transfer parameter $\overline{Y}$ on the gas flow parameter $(\dot{w}/\mu)_g$. The slope of this line, which represents the value of n in equation (14), is 0.82.

By using the slopes obtained from figures 14 and 15, the data are replotted in figure 16, the slope of which corresponds to the constant K in equation (14). The final correlation equation based on the data shown in figures 14 to 16 is

$$\overline{Y} = 0.0208 \left(\frac{\dot{w}}{\mu}\right)_g^{0.82} \Big/ \left(\frac{\dot{w}}{\mu}\right)_c^{0.66} \tag{22}$$

In this equation $(\dot{w}/\mu)$ has the dimensions of meters, while the constant 0.0208 has the dimensions of meters to the -0.16 power.

The final correlation displays good agreement with the data except at relatively high values of the abscissa which correspond to either relatively low values of coolant flow rate or to high coolant inlet temperatures. From figure 11 low flow ratios are associated with low pressure ratios, and from figure 10 low pressure ratios are associated with large changes in the flow distribution. Also, at low coolant-to-gas flow ratios, the flow distribution through a multiexit vane has been shown (fig. 11) to be substantially changed by a high coolant temperature. Therefore, these high abscissa data should not be expected to correlate as well with a different flow distribution.

$\overline{\varphi}$ correlation: It is indicated in the section ANALYSIS METHODS that the simplest correlation is that of the temperature difference ratio φ being plotted against the ratio

of coolant flow per vane to gas flow per vane $\dot{w}_c/\dot{w}_g$. Figure 17 shows the data plotted in this manner with the abscissa expressed as $\dot{w}_c/\dot{w}_g$. The agreement is good. Several observations from the trends in the data are worthy of note. If curves are drawn through each set of data points, higher gas temperatures appear to result in lower values of φ, while higher coolant temperatures appear to result in higher values of φ. These trends might be explained to a certain extent by a redistribution of the coolant flow as a result of changes in coolant temperature, coolant flow rate, and possibly other engine operating variables. As a result of the new distribution, some locations will receive more cooling while other locations receive less cooling. Since φ varies locally over the vane, the average φ will not be the same.

For the ease of usefulness of this correlation, a single least-squares curve is used to represent the data; the scatter from this line is generally within ±5 percent except for a couple of points.

Local correlations based on total coolant flow. - The installation of the 14 thermocouples at 13 locations on the midspan sections of the three middle test vanes (see fig. 6) not only allowed the determination of an average metal temperature, but also permitted study of local temperatures around the vane perimeter.

The first analysis of local midspan data is based on total coolant flow rate per vane, assuming that all 13 thermocouples are located on one composite vane and that the coolant flow rate to the five test vanes is distributed equally. Due to the difficulty in measuring local coolant temperatures in the extremely small coolant passages, the coolant inlet temperature $T_{c,i}$ is again used, and the gas-side conditions are evaluated as in the average correlation analysis.

For convenience, four thermocouples were selected for local analysis. The four were chosen to best represent the various gas-side conditions around the vane perimeter as well as the various internal cooling schemes. Future reference to local thermocouple correlations will involve thermocouple 6 at the leading-edge suction surface, thermocouple 4 at the midchord suction surface just aft of the film cooling holes, thermocouple 11 at the horizontal fin pressure surface, and thermocouple 13 at the trailing-edge pressure surface (see fig. 6).

Y_x correlation: The Y_x correlations for each of the four chosen thermocouples are shown in figure 18. For each selected thermocouple, it is necessary to determine the exponents m and n; these determinations are made in a manner similar to that used for the average correlation, except that local values of T_w are used. The particular thermocouple investigated is located on the vane sketch for each of the four selected thermocouples, and the values of m and n are also noted. For ambient cooling air (circular symbols), the data correlate well. For heated cooling air (square symbols), the data appear to scatter considerably. As the coolant flow rate decreases, the tem-

perature rise of the coolant becomes greater; and hence, the inlet coolant temperature becomes less representative of the local coolant temperature.

From figures 10 and 11 it can be seen that a smaller percentage of cooling air exits through the trailing edge for a test with heated coolant than does for a test with ambient coolant. Metal temperatures on the afterbody region should, therefore, be higher than predicted by the correlation; and so the heated cooling-air data should be above the correlation line in figure 18 rather than below it. By the same reasoning, heated cooling-air data on the leading edge should be below the line rather than above it. Therefore, nonagreement of heated cooling-air data with ambient cooling-air data, in figure 18, cannot be attributed to a change in flow distribution of the coolant.

φ_x correlation: Figure 19 shows the φ_x values plotted against the $\dot{w}_c/\dot{w}_g$ ratio for the data for the same four thermocouples considered in figure 18. Each of the thermocouples is located as shown on a sketch of the vane in figure 19, and the equation of each of the correlating curves determined by the method of least squares is given. Comparison of figures 18 and 19 indicates that the scatter in the data around the φ_x correlations is less than the scatter around the Y_x correlations. In view of this and because of the ease in applying the φ_x correlation, use of the φ_x correlation is recommended. Although only four correlations are shown in figure 19, similar correlations were found for the other thermocouple locations. The φ_x correlations for all 13 thermocouple locations are presented in table III.

Local correlations based on local flow. - Plots similar to those shown in figures 18 and 19 (based on the total coolant flow per vane) are presented in figures 20 and 21 (based on exit coolant flows). New values of the exponents m and n had to be determined for each of the four thermocouple locations selected; these locations were the same as those considered when the total flow was used. Data from thermocouples 4 and 13 were correlated with the coolant flow exiting from the trailing edge. The data of thermocouple 11 were correlated with that portion of the trailing-edge flow calculated to be flowing through the chord-wise flow passages on the pressure surface. The fourth thermocouple, the hotspot thermocouple, was located on the suction surface of the leading edge. Therefore, the flow rate through the 46 impingement holes was chosen in an attempt to correlate the leading-edge temperature data. Figures 20 and 21 show correlations essentially the same as those shown in figures 18 and 19. Little improvement is achieved when the exit coolant flow is used instead of the total coolant flow.

Comparison of Measured Average Vane Temperatures with Those Calculated from Correlations

The average measured midspan vane temperatures are compared with those calcu-

lated from the $\overline{Y}$ and $\overline{\varphi}$ correlations in figures 22 and 23, respectively. Total coolant flow per vane and inlet coolant temperature are used in determining the average vane temperatures from the correlations. The solid symbols in figures 22 and 23 represent data points that were not considered in the determination of the average correlations $\overline{Y}$ and $\overline{\varphi}$. Inspection of the figures indicates that the $\overline{\varphi}$ correlation yields results comparable to those from the $\overline{Y}$ correlation. The ease of application of the $\overline{\varphi}$ correlation and its equally good results justify its use over the $\overline{Y}$ correlation.

Comparison of Measured Local Vane Temperatures with Those Calculated from φ_x Correlations

The local measured temperatures at the midspan position were compared with the temperatures calculated by use of the local φ_x correlations which are presented in table III. With the exception of a few isolated points, error bands of ±5 percent enclose all the data.

Comparison of Empirical and Analytical Coolant Flow Rates

Figure 24 presents a comparison between empirical and analytical flow rates through the suction- and pressure-surface film cooling holes and the split trailing edge for two different engine test points. These empirical flow rates are determined with the aid of figure 10, the coolant-inlet-static-to-turbine-inlet-total pressure ratio, and the measured value of the flow rate per vane. The corresponding analytical flow rates are determined by using the previously defined flow network while forcing the sum of the analytical flow rates to equal the measured flow rate to the vane. The three shaded points in figure 24 represent one engine test point with a coolant-to-gas flow ratio of 0.07. For these conditions, the analytical flow is high through the suction-surface slot and split trailing-edge but low through the pressure-surface slot. The second set of symbols are for a coolant-to-gas flow ratio of 0.109. For this set, the analytical flow is again high through the suction-surface slot but low to the split trailing edge and high to the pressure-surface slot. In general, the agreement is very good.

Comparison of Experimental and Analytical Vane Temperatures

Experimental and analytical local vane metal temperatures for the midspan location are presented in figure 25. These analytical vane metal temperatures are obtained by

using the heat transfer coefficients and effective gas temperatures discussed in the section ANALYSIS METHODS. The chordwise temperature distributions are for the coolant-to-gas flow ratios of 0.07 and 0.109 mentioned in the previous paragraph with gas and coolant temperatures of 1453 and 296 K (2156° and 73° F), respectively, for the former flow rate and 1471 and 295 K (2188° and 72° F), respectively, for the latter. The overall agreement is fair. The analytical temperatures are generally within ±10 percent of the measured temperatures.

The agreement between the measured and analytical temperatures is fair at the impingement-cooled leading edge, good immediately downstream of the film cooling slot on the suction surface, but poor immediately downstream of the film cooling slot on the pressure surface. The film cooling correlation for the pressure surface is the suspected cause of error. This follows since the same wall-to-coolant heat transfer coefficient (eq. (12)) is used on the suction surface as on the pressure surface, and because the predicted temperature on the pressure surface is too high even though the analytical flow out of the pressure film cooling slot is slightly high.

For the chordwise passage region and the split trailing-edge region, the agreement is good on the pressure surface but only fair on the suction surface, thus casting doubt on the suction-surface gas-to-wall heat transfer coefficient. The same equations are used for both the coolant flow rate distribution and the wall-to-coolant heat transfer coefficient (eqs. (12) and (13)) on both the pressure and suction surfaces.

Analytically Improved Cooling Performance

The vane discussed was designed to operate at a maximum wall temperature of 1278 K (1840° F), an inlet coolant temperature of 922 K (1200° F), and a coolant-to-gas flow ratio of 0.05, split evenly between the leading edge and the afterbody region. Experimental flow data, extrapolated to this design point, have shown that a coolant-to-gas flow ratio of 0.05 will split 43 percent to the leading-edge region (18 percent to the suction-surface film cooling holes and 25 percent to the pressure-surface film cooling holes) and 57 percent to the afterbody region. Such an adverse flow distribution would have resulted in leading-edge wall temperatures in excess of 1278 K (1840° F) had the vane actually been tested at any gas temperature above 1348 K (1967° F).

The midspan temperature distributions in figure 25 show that the chordwise-finned region is overcooled relative to the trailing edge; the trailing edge is overcooled relative to the leading-edge pressure surface; and the leading-edge pressure surface is overcooled relative to the leading-edge suction surface.

This vane design could be improved by changing certain critical dimensions so that a greater proportion of the coolant is distributed to the hotter leading-edge area. The

critical dimensions which would change are the trailing-edge slot width, the impingement nozzle diameters, and the film cooling hole diameters.

The vane can be further improved by changes in design other than just redistributing flow by changing critical dimensions. One such example would be to optimize the leading-edge impingement geometry. Reference 17 states that maximum heat transfer occurs when the spacing between the semicylinder and a linear array of circular jets is approximately two equivalent slot widths, whereas the original vane has a spacing of 10.7 slot widths.

Another change which would improve the design is the extension of the chordwise passages closer to the leading-edge region. Increasing the leading-edge flow from the original 43 percent so as to decrease the leading-edge temperature and the temperature gradient caused the unfinned portion of the vane to be the afterbody hotspot. Hence, extending fins to this region will reduce this hotspot temperature.

Further changes in the basic geometry of the vane can also be made which will tend to improve the vane. Bypassing the chordwise passages with approximately 16 percent of the afterbody cooling air directly to the split trailing edge will decrease the gradient by increasing the minimum temperature along the finned midchord region. The temperature of the finned area will increase because of less coolant flow through the finned passages. This design change has the added benefit of decreasing the overall pressure drop across the vane.

Calculated temperature distributions for both the original and revised vanes are presented in figure 26. The temperature distribution for the original vane is obtained by evaluating the local temperature difference ratios based on the total coolant flow per vane, the constants of which are in table III. The temperature distribution for the revised vane is obtained from similar temperature difference ratios based on local flow rates.

For a turbine inlet total gas temperature of 1509 K (2257° F), a coolant temperature of 922 K (1200° F), and a coolant-to-gas flow ratio of 0.05, the calculated maximum temperature of the revised vane is 1278 K (1840° F). These calculations showed that the leading-edge temperature is reduced 134 K (241° F) and the average temperature is reduced 2 K (3.6° F) relative to the original design. The maximum to minimum difference is 294 K (529° F) on the original design compared to 152 K (274° F) on the revised design. The required ratio of coolant inlet pressure to turbine inlet pressure, which is necessary for the vane to pass a 0.05 coolant-to-gas flow ratio at 922 K (1200° F), will be reduced from 1.11 to 1.00. The flow distribution will change to 36.4 percent to the suction-surface film cooling holes, 26.2 percent to the pressure-surface film cooling holes, and 37.4 percent to the afterbody region compared with 18, 25, and 57 percent, respectively. Both the original and revised geometry, temperatures, and flow distributions are presented in table IV.

Allowable Hotspot Turbine Inlet Temperature

As was mentioned earlier, the complete stator assembly consisted of 67 slave vanes and five test vanes. Both of these configurations were described in the section APPARATUS.

Vanes of the slave configuration have been investigated in a high-temperature cascade as described in reference 1 and also in the test vane positions of the engine, as have several other stator vane configurations. This slave vane configuration has been shown, in unpublished data, to have the most effective cooling configuration of those stator vanes recently tested at Lewis.

For both the slave and test configurations investigated in the engine, hotspot local metal temperatures have been correlated in the form of temperature difference ratios similar to those of figure 19. From such a correlation, a hotspot turbine inlet temperature may be associated with a given coolant-to-gas flow ratio for a fixed coolant inlet temperature and a maximum allowable airfoil metal temperature.

These relations between calculated hotspot turbine inlet temperature and coolant-to-gas flow ratio are shown in figure 27. The comparison shows that for a coolant-to-gas flow ratio of 0.05, a coolant inlet temperature of 922 K (1200° F), and an allowable metal temperature of 1278 K (1840° F) the revised vane configuration may be operated in the engine at a hotspot turbine inlet temperature of 1509 K (2257° F), which is 30 K (54° F) higher than that of the slave vane configuration. For similar conditions the revised chordwise-finned vane can be operated at a hotspot gas temperature 160 K (288° F) higher than can the vane with the original configuration.

The cooling-air temperature of 922 K (1200° F) approximates the coolant inlet temperature for a turbojet engine during supersonic cruise. For a ten-to-one compressor pressure ratio, which is representative of a sea-level takeoff condition for a supersonic cruise turbojet engine, the corresponding compressor exit temperature would be 616 K (648° F), assuming normal compressor efficiency and standard-day inlet conditions. This temperature approximates the compressor bleed temperature which is used for cooling the vane at sea-level takeoff conditions.

The circular point in figure 27 represents the calculated allowable hotspot turbine inlet temperature for the modified chordwise-finned vane during a sea-level takeoff. For an allowable metal temperature of 1278 K (1840° F), a coolant inlet temperature of 616 K (648° F), and a coolant-to-gas flow ratio of 0.05, the vane can withstand a hotspot gas temperature of 1735 K (2663° F).

Advanced Bonding Techniques

Because the vane configuration was evolved primarily to study heat transfer charac-

teristics, the development of a practical production-type fabrication procedure for the configuration was not within the scope of this investigation. It should be noted, however, that studies of advanced bonding techniques for joining finned shells to supporting struts for the possible fabrication of this type of vane have been made on NASA contracts and are reported in references 18 and 19. Also, unpublished information that has become available since the start of this program indicates that several fabricators may have the capability of casting the outer shells and fins as well as the orifice partition of this type of vane configuration in one piece.

SUMMARY OF RESULTS

An air-cooled turbine vane configuration was investigated for its cooling performance in a turbojet engine. The vanes were operated at turbine inlet gas temperatures to about 1644 K (2500° F), at coolant temperatures to 700 K (800° F), and coolant-to-gas flow ratios to 0.187. The vane configuration had an impingement-cooled leading edge; the region immediately aft of the leading edge was film cooled; the midchord and trailing-edge regions were convection cooled. The midchord convection cooling was enhanced by the use of a large number of small chordwise passages. The coolant used for the midchord and trailing-edge regions was ejected from the vane through passages in the extreme trailing edge of the vane airfoil. The results are summarized as follows:

1. The average and local midspan vane wall temperatures were successfully correlated by means of the temperature difference ratio φ as a function of the coolant-to-gas flow ratio. (The temperature difference ratio considers the effective gas temperature, the cooling-air inlet temperature to the vane, and the vane wall temperature.)

2. Equations that fit the correlated data were determined and the measured midspan wall temperatures generally differed by no more than ±5 percent from those determined by the correlation equations.

3. Measured midspan vane wall temperatures generally differed by no more than ±10 percent from those obtained by analytical equations.

4. For a vane having multiple exits for the cooling air, the coolant flow distribution was found to be a function of the coolant temperature.

5. A method is presented for determining the coolant flow distribution through a multiexit turbine vane using cold-flow calibration curves and engine data.

6. The design concept of small chordwise fins, which significantly increases the effective heat transfer area, is shown to be especially effective from a heat transfer standpoint. However, because of excessively high local leading-edge temperatures, high thermal gradients between the leading edge and midchord regions, and objectionably high pressure drop, the original vane design is not practical.

7. The design of the original vane was modified to decrease the leading-edge hotspot temperature, the temperature gradient from the leading edge to the midchord region, and the pressure drop across the vane.

A comparison of some pertinent temperatures and coolant pressure requirements for the original vane and the revised design are shown in the following table:

	Original vane	Revised vane
Turbine inlet total gas temperature, K (^{o}F)	1509 (2257)	1509 (2257)
Cooling-air inlet temperature, K (^{o}F)	922 (1200)	922 (1200)
Ratio of cooling-air flow to gas flow	0.05	0.05
Calculated hotspot vane metal temperatures, K (^{o}F)	1412 (2081)	1278 (1840)
Calculated average chordwise vane temperature at midspan, K (^{o}F)	1229 (1752)	1227 (1749)
Calculated difference between maximum and minimum midspan temperature, K (^{o}F)	294 (529)	152 (274)
Coolant-inlet-to-turbine-inlet pressure ratio necessary to pass design flow rate	1.1	1.0

Lewis Research Center,
National Aeronautics and Space Administration,
and
U.S. Army Air Mobility R&D Laboratory,
Cleveland, Ohio, January 18, 1972,
764-74.

APPENDIX - SYMBOLS

A	coefficient in table III
B	exponent in table III
C_2	constant
c_p	specific heat
D	leading-edge diameter of vane
D_h	hydraulic diameter
F	$\bar{h}_g S_g / \dot{w}_c c_{p,c}$
g_c	dimensional conversion factor
h	heat transfer coefficient
J	mechanical equivalent of heat
K, K_1	constants
k	thermal conductivity
L	surface distance from leading edge to trailing edge
L_{fin}	effective fin width
l	maximum distance from stagnation line over which impingement cooling is effective
M	$\rho_c v_c / \rho_g v_g$
m	exponent
m_{fin}	surface-to-surface spacing between fins
Nu	Nusselt number
n	exponent
P	pressure
Pr	Prandtl number
p	exponent
q	exponent
Re	Reynolds number
S	heat transfer surface area
s	slot width

T	temperature
v	velocity
$\dot{w}$	flow rate
x	distance from film cooling hole or distance from stagnation point
Y	$\left[(1 - \varphi)/\varphi\right] \left[\left(Pr_c^{1/3} k_c\right) \Big/ \left(Pr_g^{1/3} k_g\right)\right]$
δ	$P_{c,i} \Big/ (1.013\ N/m^2)$
η_f	$\left(T_{ge} - T_{aw}\right) \Big/ \left(T_{ge} - T_{c,o}\right)$
η_t	$\left(\bar{T}_{c,o} - T_{c,i}\right) \Big/ \left(\bar{T}_w - T_{c,i}\right)$
θ	angle measured from stagnation point
θ_{atm}	$T_{c,i} \Big/ 288.2\ K$
Λ	recovery factor
μ	viscosity
ρ	density
τ_{fin}	fin thickness
φ	$\left(T_{ge} - T_w\right) \Big/ \left(T_{ge} - T_c\right)$
φ_{fin}	$\left(2h_i \Big/ k_w \tau_{fin}\right)^{1/2}$

Subscripts:

aw	adiabatic wall
c	coolant
D	leading-edge diameter of test vane
D_h	based on hydraulic diameter
g	gas
ge	effective gas
i	in
n	evaluated at impingement hole diameter and velocity
o	out
ref	reference
s	slot

st static

Ti turbine inlet total

w wall

x distance from leading-edge stagnation point

y distance along vane span

Superscripts:

' total

— average

REFERENCES

1. Gladden, Herbert J.; Gauntner, Daniel J.; and Livingood, John N. B.: Analysis of Heat-Transfer Tests of an Impingement-, Convection-, and Film-Cooled Vane in a Cascade. NASA TM X-2376, 1971.

2. Calvert, Howard F.; Cochran, Reeves P.; Dengler, Robert P.; Hickel, Robert O.; and Norris, James W.: Turbine Cooling Research Facility. NASA TM X-1927, 1970.

3. Gladden, Herbert J.; Dengler, Robert P.; Evans, David G.; and Hippensteele, Steven A.: Aerodynamic Investigation of Four-Vane Cascade Designed for Turbine Cooling Studies. NASA TM X-1954, 1970.

4. Clark, John S.; Richards, Hadley T.; Poferl, David J.; and Livingood, John N. B.: Coolant Pressure and Flow Distribution Through an Air-Cooled Vane for a High-Temperature Gas Turbine. NASA TM X-2028, 1970.

5. Gladden, Herbert J.; Livingood, John N. B.; and Gauntner, Daniel J.: Comparison of Temperature Data from a Four-Vane Static Cascade and a Research Gas Turbine Engine for a Chordwise-Finned, Impingement- and Film-Cooled Vane. NASA TM X-2477, 1971.

6. Katsanis, Theodore: Fortran Program for Calculating Transonic Velicities on a Blade-to-Blade Stream Surface on a Turbomachine. NASA TN D-5427, 1969.

7. Katsanis, Theodore; and Dellner, Lois T.: A Quasi-Three-Dimensional Method for Calculating Blade Surface Velocities for an Axial Flow Turbine Blade. NASA TM X-1394, 1967.

8. Kreith, Frank: Principles of Heat Transfer. International Textbook Co., 1958.

9. Rohsenow, Warren H.; and Choi, Harry Y.: Heat, Mass, and Momentum Transfer. Prentice-Hall, Inc., 1961.

10. Eckert, E. R. G.; and Drake, Robert M., Jr.: Heat and Mass Transfer. Second ed., McGraw-Hill Book Co., Inc., 1959.

11. Burggraf, F.; Murtaugh, J. P.; and Wilson, M. E.: Design and Analysis of Cooled Turbine Blades. Part 1: Leading and Trailing Edge Configurations. Rep. R68AEG101, General Electric Co. (NASA CR-54513), Jan 1, 1967.

12. Jenkins, D. E.; and Metzger, C. W.: Local Heat Transfer Characteristics of Concave Cylindrical Surfaces Cooled by Impinging Slot Jets and Lines of Circular Jets with Spacing Ratios 1.25 to 6.67. TR No. 694, Arizona State Univ., May 1969.

13. Burggraf, F.: Average Heat Transfer Coefficients with a Row of Air Jets Discharging into a Half Cylinder. M.S. Thesis, Univ. Cincinnati, 1967.

14. McAdams, William H.: Heat Transmission. Third ed., McGraw-Hill Book Co., Inc., 1954.

15. Livingood, John N. B.; and Brown, W. Byron: Analysis of Spanwise Temperature Distribution in Three Types of Air-Cooled Turbine Blade. NACA TR 994, 1950.

16. Stepka, Francis S.: Considerations of Turbine Cooling Systems for Mach 3 Flight. NASA TN D-4491, 1968.

17. Metzger, D. E.; Yamashita, T.; and Jenkins, C. W.: Impingement Cooling of Concave Surfaces with Lines of Circular Air Jets. Paper 68-WA/GT-1, ASME, Dec. 1968.

18. Kaufman, A.; Berry, T. F.; and Meiners, K. E.: Joining Techniques for Fabrication of Composite Air-Cooled Turbine Blades and Vanes. Paper 71-GT-32, ASME, Mar. 1971.

19. Wilbers, L. G.; Berry, T. F.; Kutchera, R. E.; and Edmonson, R. E.: Development of the Activated Diffusion Brazing Process Fabrication of Finned Shell to Strut Turbine Blades. General Electric Co. (NASA CR-72844), Nov. 1971.

TABLE I. - STATIC PRESSURE TAP LOCATIONS ON CALIBRATION VANES

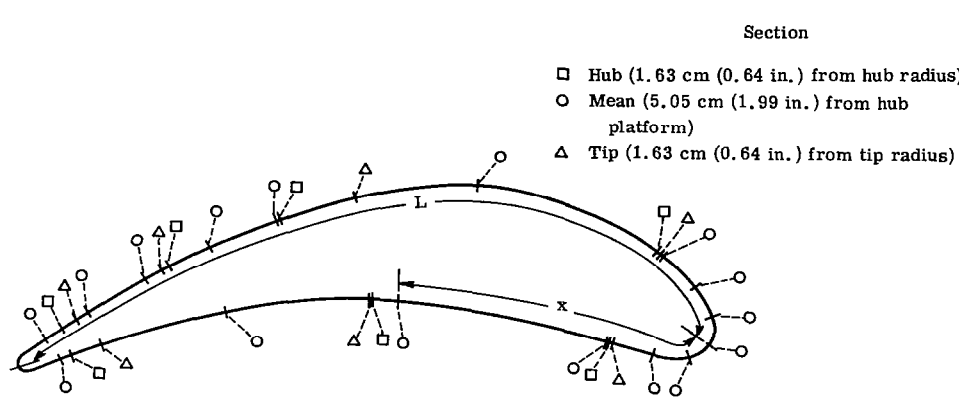

Suction surface[a]			Pressure surface[a]		
Surface distance, x		Dimensionless surface distance, x/L	Surface distance, x		Dimensionless surface distance, x/L
cm	in.		cm	in	
Hub section					
Vane surface distance from leading edge to trailing edge, L = 7.26 cm (2.859 in.)			Vane surface distance from leading edge to trailing edge, L = 6.58 cm (2.591 in.)		
1.02	0.401	0.140	0.950	0.374	0.144
4.51	1.777	.622	3.15	1.241	.479
5.59	2.201	.770	5.941	2.339	.903
6.69	2.634	.921	-----	-----	-----
Mean section					
Vane surface distance from leading edge to trailing edge, L = 7.27 cm (2.861 in.)			Vane surface distance from leading edge to trailing edge, L = 6.53 cm (2.571 in.)		
0	0	0	0.239	0.094	0.037
.257	.101	.035	.556	.219	.085
.554	.218	.076	.993	.391	.152
.940	.370	.129	2.924	1.151	.448
2.766	1.089	.381	4.514	1.777	.691
4.562	1.796	.628	6.068	2.389	.929
5.197	2.046	.715	-----	-----	-----
5.832	2.296	.803	-----	-----	-----
6.403	2.521	.881	-----	-----	-----
6.848	2.696	.942	-----	-----	-----
Tip section					
Vane surface distance from leading edge to trailing edge, L / 7.30 cm (2.872 in.)			Vane surface distance from leading edge to trailing edge, L = 6.51 cm (2.563 in.)		
0.940	0.370	0.129	0.940	0.370	0.144
3.807	1.499	.522	3.211	1.264	.493
5.636	2.219	.773	5.682	2.237	.873
6.515	2.565	.893	-----	-----	-----

[a]Leading-edge tap and all pressure-surface taps located on one vane; all suction-surface taps located on second vane.

TABLE II. - SUMMARY OF ENGINE OPERATING CONDITIONS AND VANE TEMPERATURES

Symbol[a]	Series	Run	Turbine stator inlet temperature, K	Gas flow per vane channel, kg/sec	Vane coolant-to-gas-flow ratio	Average vane inlet cooling-air temperature, K	Vane metal temperature, K																							
							Thermocouple[b]																							
							7b	5	3	2	13	11	9	7a	15	19	14	12	10	8	20a	6	4	1	23	17	21	22	16	18	20b
	1	5	1040	0.427	0.083	299	831	664	510	616	607	487	646	786	596	584	553	734	478	552	836	827	584	660	577	515	642	446	738	479	798
		6	1037	.427	.072	299	842	683	518	625	628	503	668	806	610	596	563	759	509	578	856	843	602	668	606	546	671	464	754	486	813
		9	1028	.43	.052	301	865	723	537	642	671	548	717	851	642	640	583	817	614	628	902	877	631	690	660	628	872	517	794	503	854
		15	1045	.43	.061	300	870	717	534	642	656	529	708	837	628	614	576	795	557	609	879	873	622	692	643	588	766	496	778	494	837
	2	16	1333	0.46	0.110	299	1038	807	584	728	682	534	767	954	697	704	640	868	506	621	1052	1029	689	801	626	558	756	485	864	558	1031
		18	1335	↓	.083	299	1075	854	613	764	758	588	836	998	750	721	679	932	571	682	1103	1076	722	821	717	633	843	544	917	583	1082
		20	1346		.075	294	1082	868	621	771	777	605	853	1018	761	733	686	957	607	707	1104	1081	733	829	746	663	874	569	929	583	1091
		21	1343		.067	290	1093	886	631	780	799	627	874	1040	773	749	692	984	654	732	1118	1096	749	843	783	701	938	600	946	584	1111
	3	40	1392	0.31	0.134	296	1007	791	569	711	637	504	746	951	693	688	638	862	500	591	1003	1016	694	782	564	553	715	446	920	538	991
		42	1397	.30	.108	296	1042	834	596	748	698	542	800	988	744	705	673	912	529	643	1052	1061	718	831	635	589	781	483	954	557	1019
		44	1329	.30	.080	296	1023	842	602	747	733	574	814	982	760	707	684	924	583	681	1016	1030	713	804	680	649	808	532	981	568	1024
		47	1356	.32	.049	297	1130	952	669	817	851	698	946	1108	844	852	743	1071	833	818	1134	1123	797	987	797	843	1049	652	1079	617	1131
	4	49	1490	0.33	0.130	295	1082	854	612	763	683	528	809	1030	734	717	669	937	528	641	1072	1064	720	822	608	565	761	470	972	563	1067
		51	1469	↓	.109	296	1099	876	619	785	723	555	834	1039	764	725	689	957	546	677	1086	1086	729	848	653	592	801	495	993	572	1069
		53	1453		.070	296	1177	979	692	852	878	707	972	1151	866	848	760	1107	818	829	1196	1179	821	914	852	829	1094	658	1104	619	1163
		55	1458		.053	298	1201	1000	712	874	902	727	991	1177	886	879	778	1133	842	851	1219	1202	838	932	865	846	1112	666	1118	741	1180
	5	101	1579	0.37	0.187	294	(c)	874	574	724	604	486	873	1041	736	743	663	932	508	558	1139	1104	722	778	525	530	784	430	968	562	1086
		102	1578	.38	.144	294		923	606	776	672	519	928	1096	784	753	712	994	537	633	1188	1148	747	837	599	568	856	463	1032	583	1136
		104	1568	.37	.101	294		994	655	843	778	583	1005	1135	848	767	758	1055	589	724	1236	1191	780	892	722	632	947	538	1082	611	1198
		105	1581	.37	.083	295		1045	694	889	844	636	1064	1192	900	798	799	1122	667	791	1268	1229	811	924	799	689	1007	594	1139	629	1234
	6	227	1368	0.28	0.110	478		953	687	804	757	646	891	1013	834	824	762	717	672	961	1136	1104	802	851	710	701	903	596	989	636	1034
		228	1366	.28	.096	478		976	699	821	782	660	912	1029	851	831	776	746	684	984	1143	1117	811	868	740	712	922	613	1006	642	1052
		229	1364	.28	.081	478		1005	716	842	816	683	944	1050	869	839	791	787	707	1016	1153	1121	821	891	783	738	948	640	1026	647	1058
	7	230	1362	0.31	0.041	477		1094	783	912	926	789	1010	1121	956	949	852	910	933	1164	1216	1197	901	967	894	907	1165	748	1134	679	1142
		231	1399	.31	.047	478		1102	784	913	928	782	1026	1166	964	924	854	907	885	1150	1213	1212	903	978	907	883	1133	753	1127	682	1149
		233	1356	.29	.079	479		1018	723	851	828	692	956	1068	886	848	803	800	712	1024	1169	1149	834	906	796	753	962	648	1040	653	1080
	8	247	1361	0.29	0.109	456		960	875	794	743	628	892	1018	838	847	754	717	641	984	1155	1125	791	843	698	691	904	579	1000*	624	1054
		248	1372	.30	.042	457		1101	772	899	926	786	1024	1189	962	969	844	906	901	1181	1221	1239	928	969	889	895	1165	744	1143*	673	1168
		251	1375	.32	.021	470		1291	938	978	1021	951	1291	1306	1224	1159	1006	992	1176	1323	1302	1354	1177	1053	954	1222	1308	820	1263*	754	1264
	9	253	1379	0.29	0.174	694		1010	832	886	861	812	918	1061	926	1003	875	859	833	1029	1175	1150	919	923	834	874	969	774	1100*	797	1069
		254	1375	.30	.099	686		1060	856	934	914	835	979	1105	962	986	903	897	841	1083	1201	1191	938	976	874	877	1019	788	1128*	799	1118
		256	1370	.31	.053	673		1125	881	978	989	879	1061	1163	1011	997	935	973	903	1153	1223	1214	963	1034	974	941	1091	858	1173*	804	1153
		257	1368	.31	.038	662		1163	902	996	1025	916	1089	1226	1043	1049	953	1017	1009	1226	1246	1250	1002	1053	997	1003	1204	885	1208*	811	1193
		258	1377	.32	.024	647		1239	956	1024	1071	986	1248	1306	1188	1179	1020	1043	1156	1323	1300	1335	1142	1094	1027	1155	1304	914	1176*	837	1276
	10	271	1656	0.36	0.178	677	↓	999	615	777	642	508	874	1234	919	872	718	601	518	1168	1354	1243	711	801	599	561	942	462	1177*	542	1256

[a]See figs. 16, 17, 19, and 21 to 23.

[b]Thermocouple numbers and locations are defined in fig. 6.

[c]Thermocouple failed.

TABLE III. - LOCAL φ CORRELATION EQUATIONS

$$\left[\varphi_x = 1 \Big/ \left[1 + A\left(\frac{\dot{w}_c}{\dot{w}_g}\right)^{-B}\right]\right]$$

Thermocouple	A	B
1	0.2753	0.48
2	.2643	.41
3	.1187	.49
4	.1304	.67
5	.1648	.83
6	.2367	1.02
7	.2628	.85
8	.1215	1.08
9	.1252	.87
10	.0180	1.25
11	.0470	.79
12	.0809	.77
13	.1036	.74

TABLE IV. - SUMMARY OF DIFFERENCES BETWEEN ORIGINAL AND REVISED VANE DESIGNS

	Original design	Revised design
Trailing-edge flow width, cm (in.)	0.076 (0.030)	0.064 (0.025)
Impingement hole diameter, cm (in.)	0.127 (0.050)	0.186 (0.073)
Film cooling suction-surface hole diameter, cm (in.)	0.064 (0.025)	0.102 (0.040)
Film cooling pressure-surface hole diameter, cm (in.)	0.071 (0.028)	0.099 (0.039)
Percent flow through split trailing edge	57	37.4
Percent flow through impingement holes	43	62.6
Percent flow through suction-surface film cooling holes	18	36.4
Percent flow through pressure-surface film cooling holes	25	26.2
Hotspot vane temperature, K (^{o}F)	1412 (2081)	1278 (1840)
Average vane temperature, K (^{o}F)	1229 (1752)	1227 (1749)
Difference between maximum and minimum temperatures, K (^{o}F)	294 (529)	152 (274)
Coolant-inlet-to-turbine-inlet pressure ratio necessary to pass design flow rate	1.1	1.0

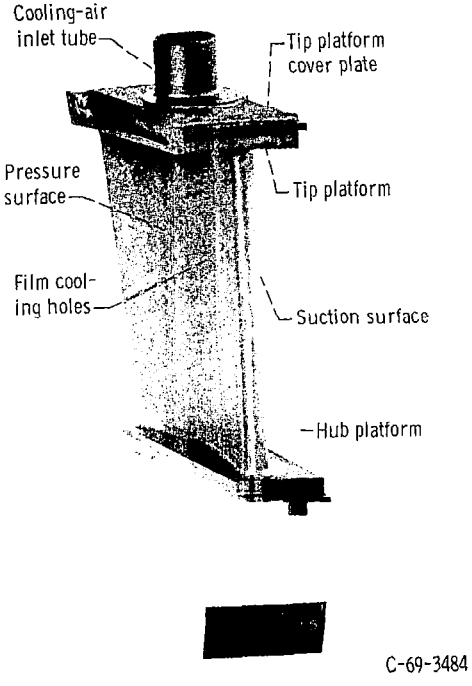

Figure 1. - Test vane assembly.

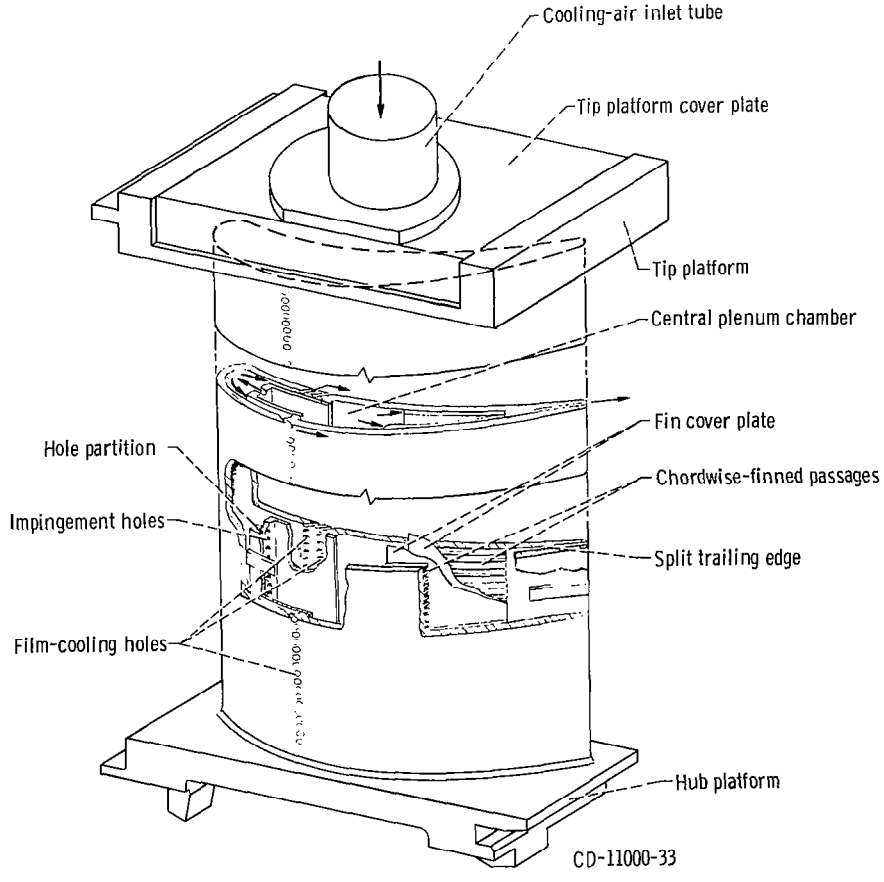

Figure 2. - Schematic diagram of test vane.

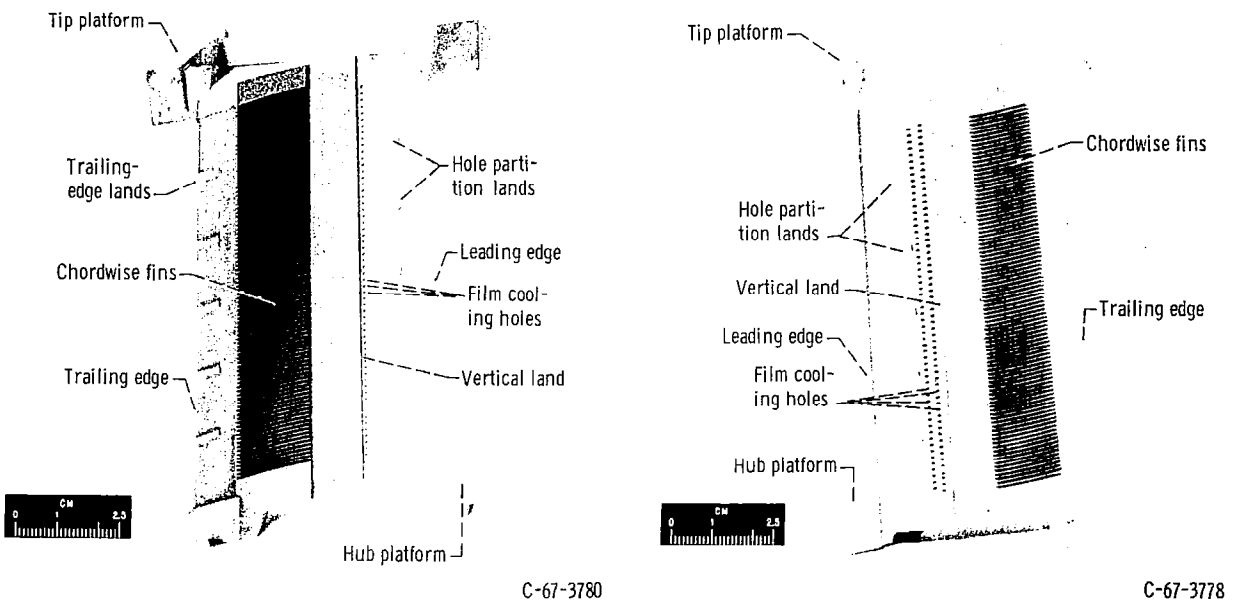

(a) Suction-surface subassembly.

(b) Pressure-surface subassembly.

Figure 3. - Internal (coolant side) surfaces of vane subassemblies.

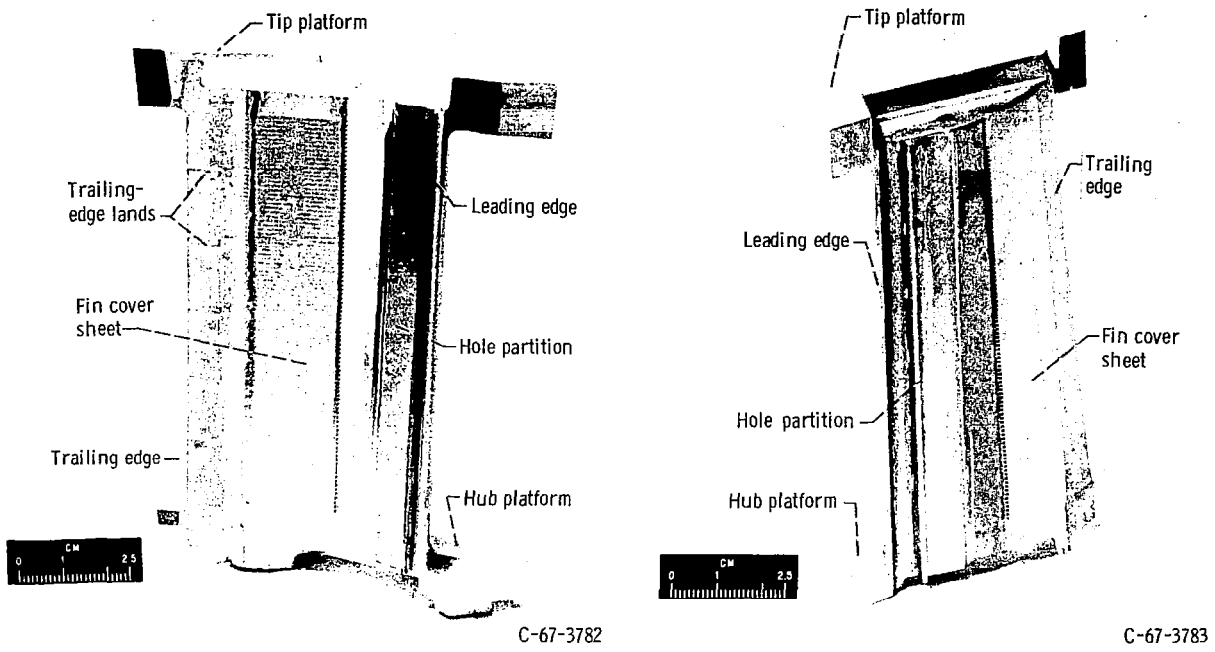

(a) Suction-surface subassembly.

(b) Pressure-surface subassembly.

Figure 4. - Internal (coolant side) surface of vane subassembly with fin cover sheet and orifice partition brazed in place.

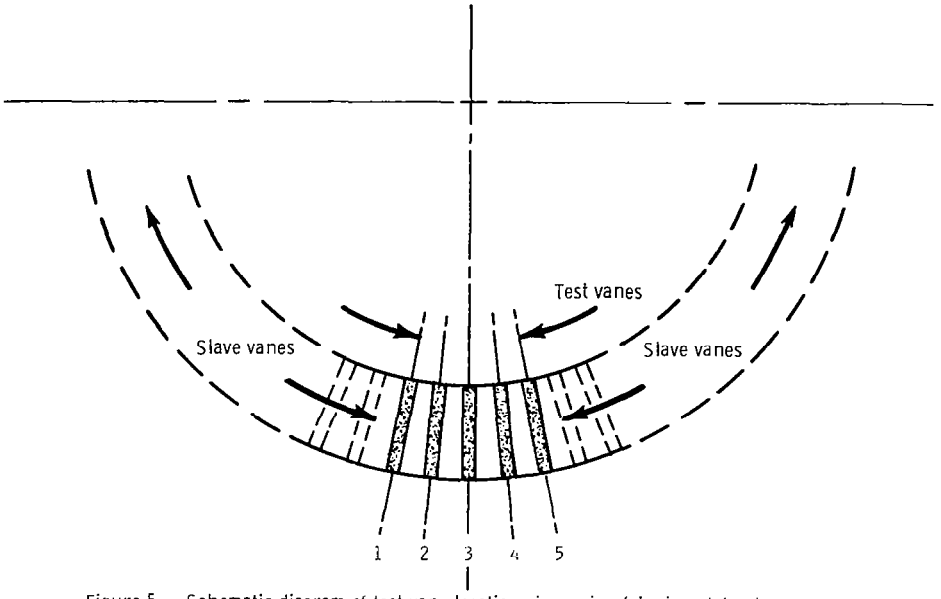

Figure 5. - Schematic diagram of test vane locations in engine (viewing stator from rear of engine).

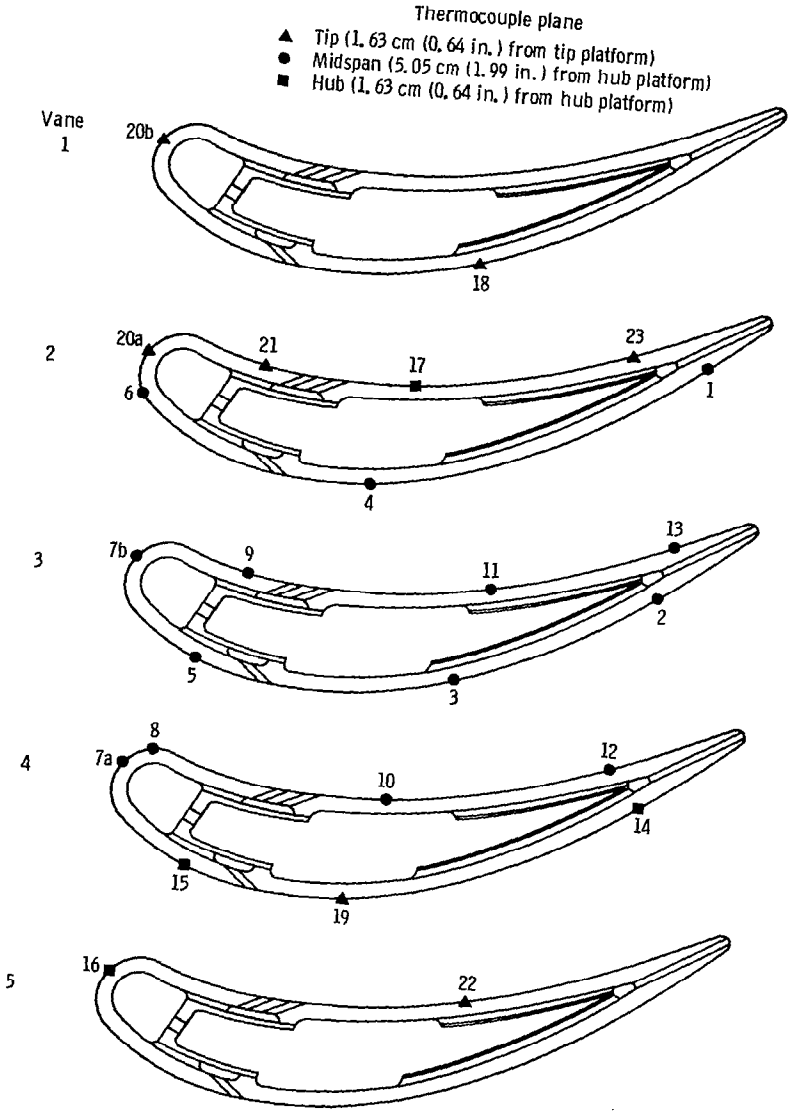

Figure 6. - Thermocouple locations on test vanes.

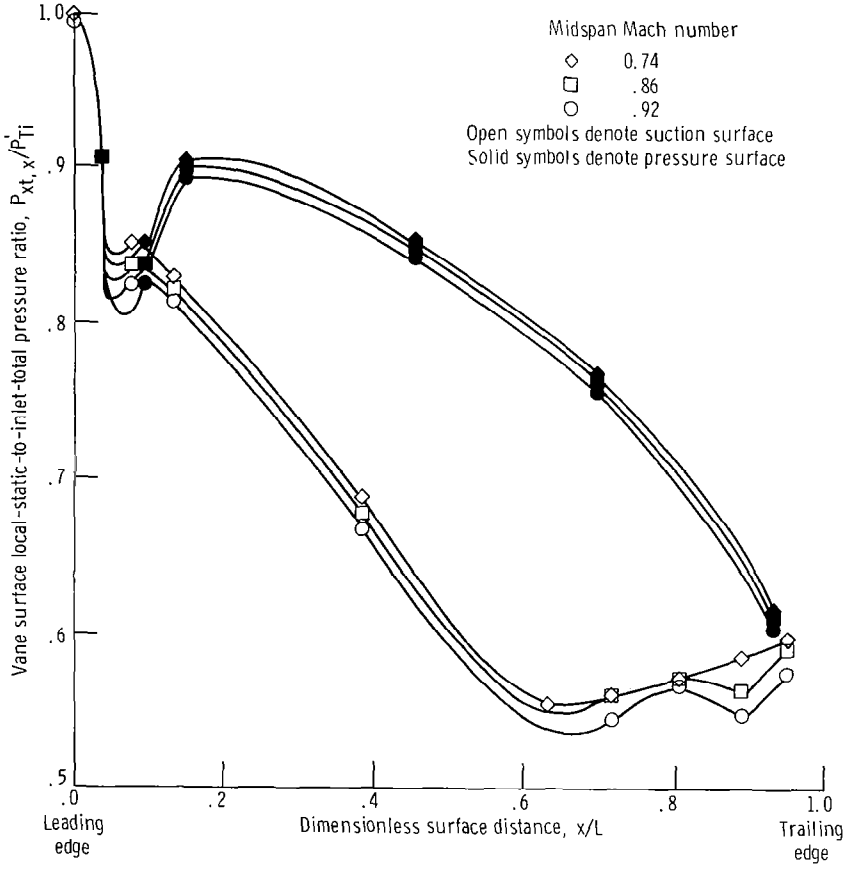

Figure 7. - Experimental midspan distribution of vane surface-pressure ratios obtained from turbojet engine tests for exit midspan Mach number of 0.74, 0.86, and 0.92.

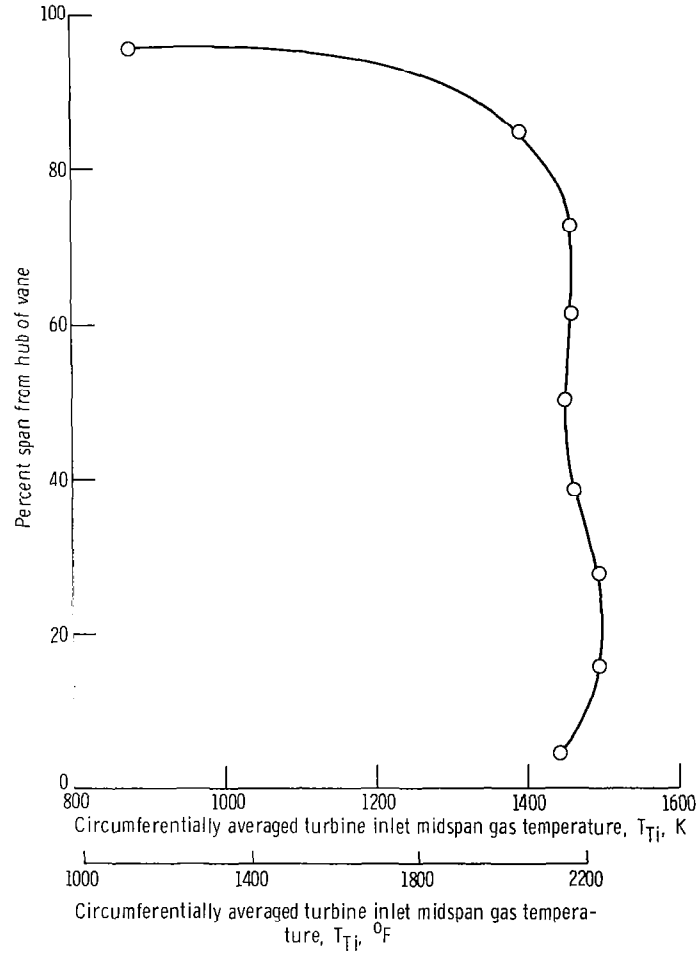

Figure 8. - Typical radial gas temperature profile at turbine inlet.

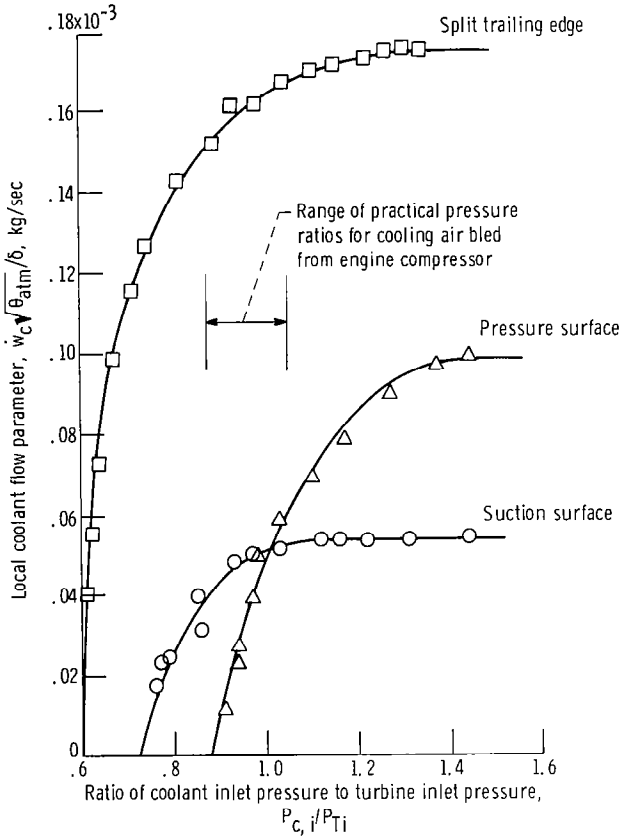

Figure 9. - Local coolant flow parameter through each of three vane exits as function of ratio of coolant inlet pressure to turbine inlet pressure.

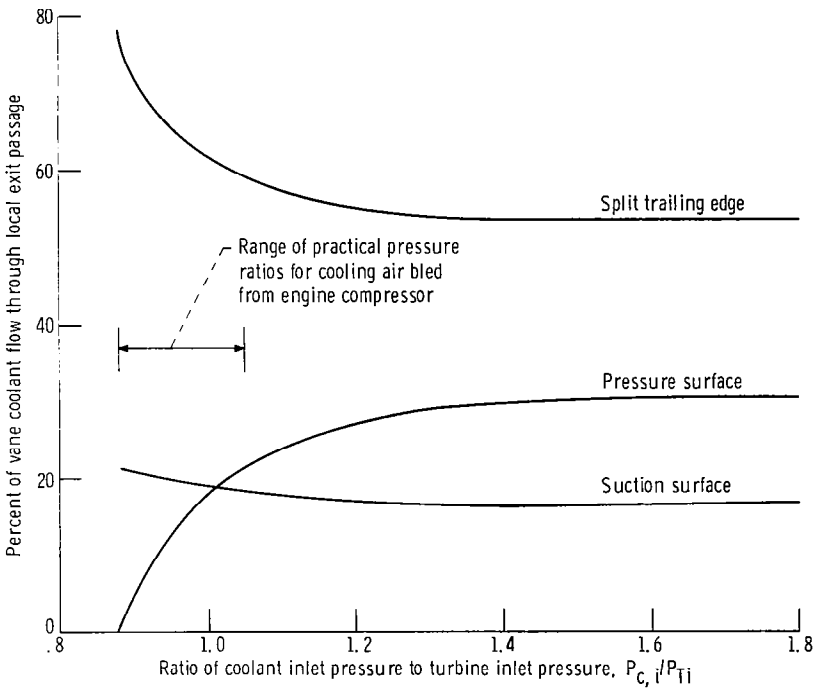

Figure 10. - Percent of coolant per vane through each exit as function of pressure ratio.

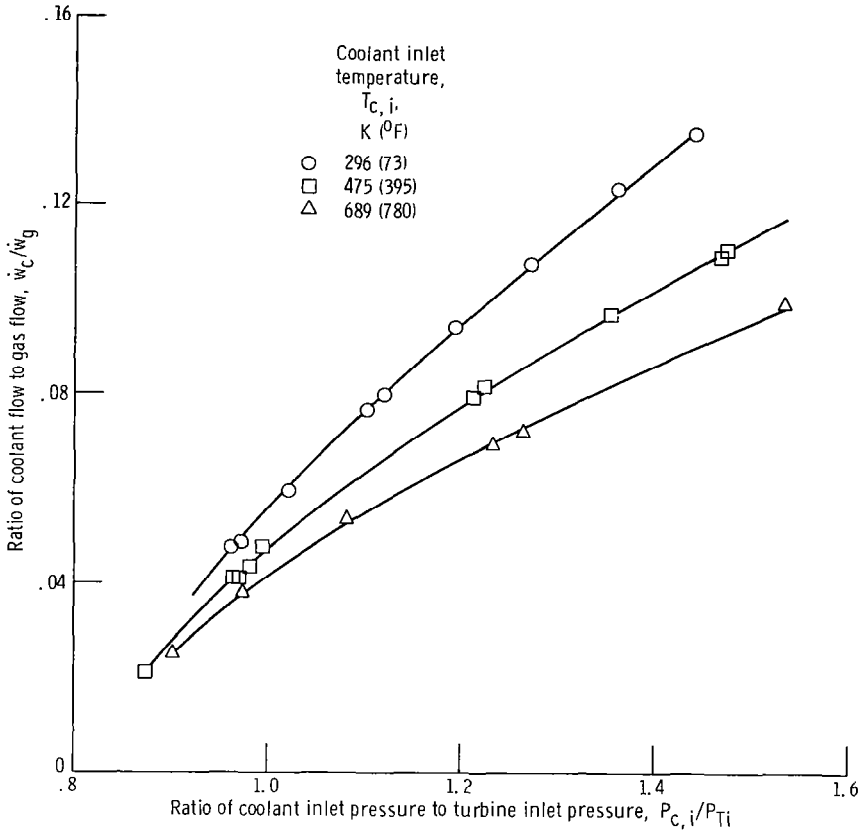

Figure 11. - Coolant flow ratio as function of pressure ratio with coolant temperature as a parameter.

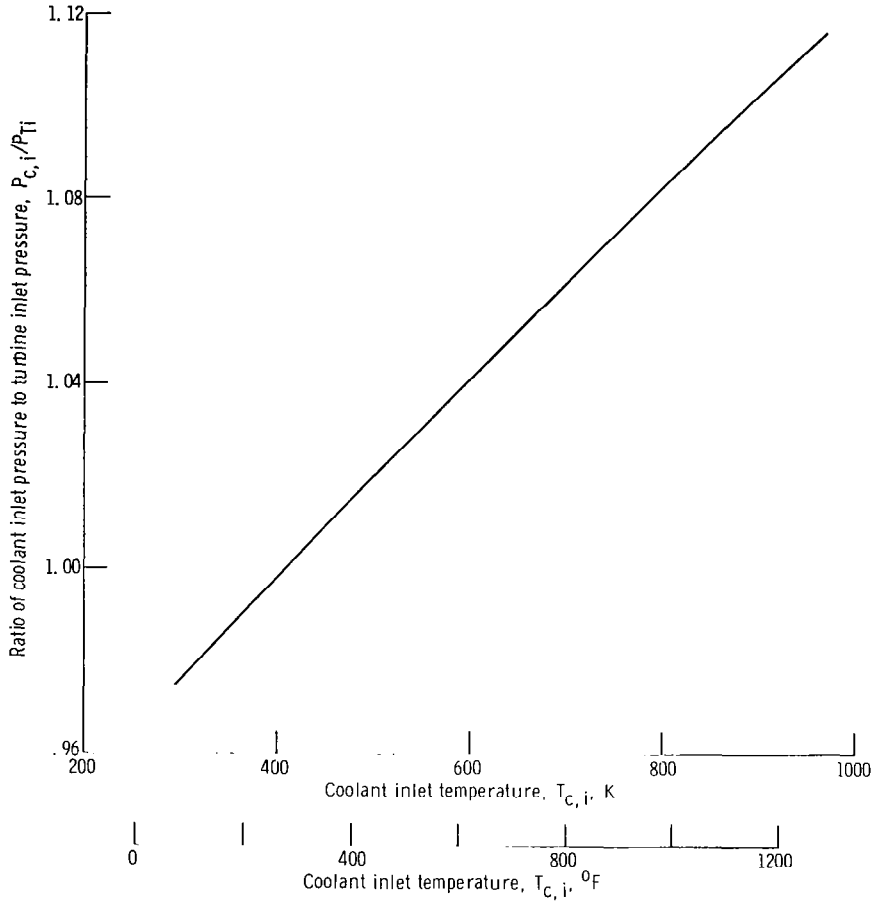

Figure 12. - Pressure ratio as function of coolant inlet temperature for ratio of coolant flow to gas flow of 0.05.

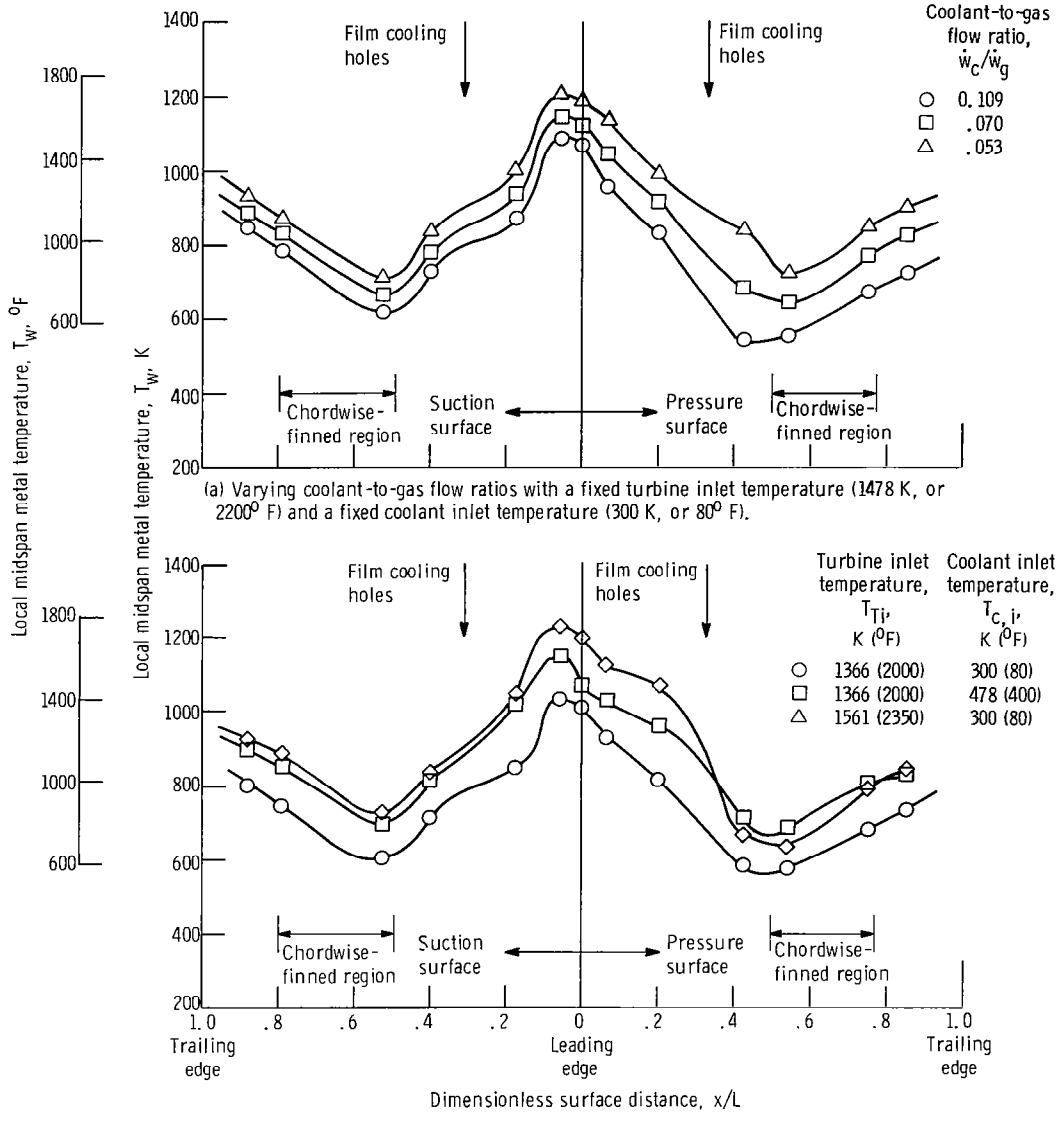

(a) Varying coolant-to-gas flow ratios with a fixed turbine inlet temperature (1478 K, or 2200° F) and a fixed coolant inlet temperature (300 K, or 80° F).

(b) Varing gas and coolant temperatures with a fixed coolant-to-gas flow ratio (0.08).

Figure 13. - Chordwise experimental vane temperature distribution for the midspan.

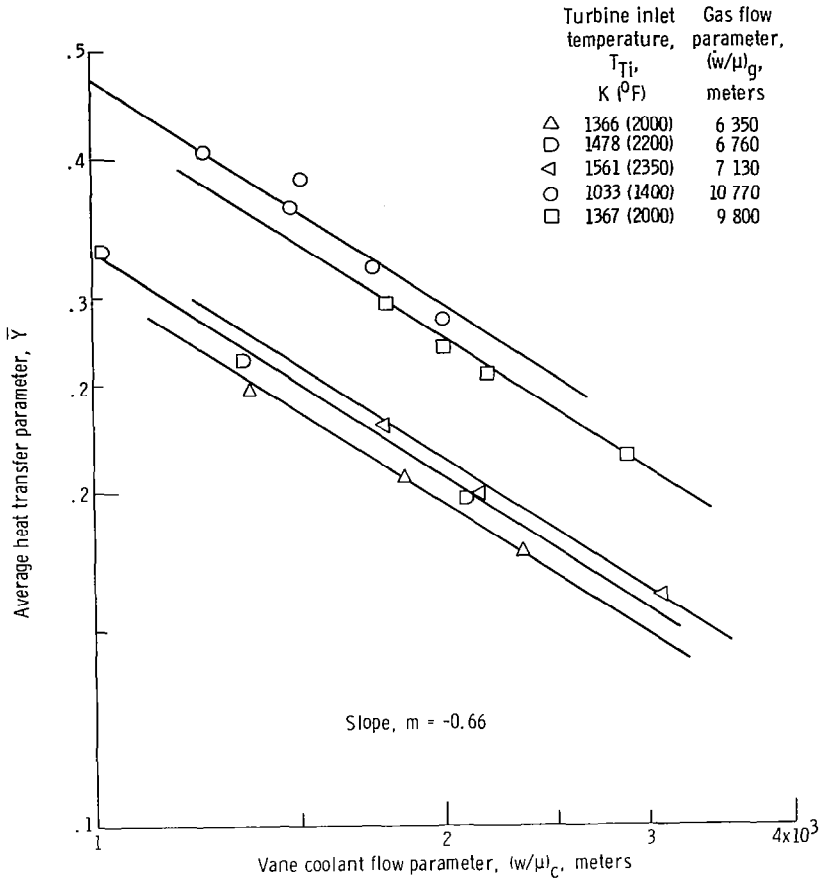

Figure 14. - Representative figure showing determination of exponent m of equation (14).

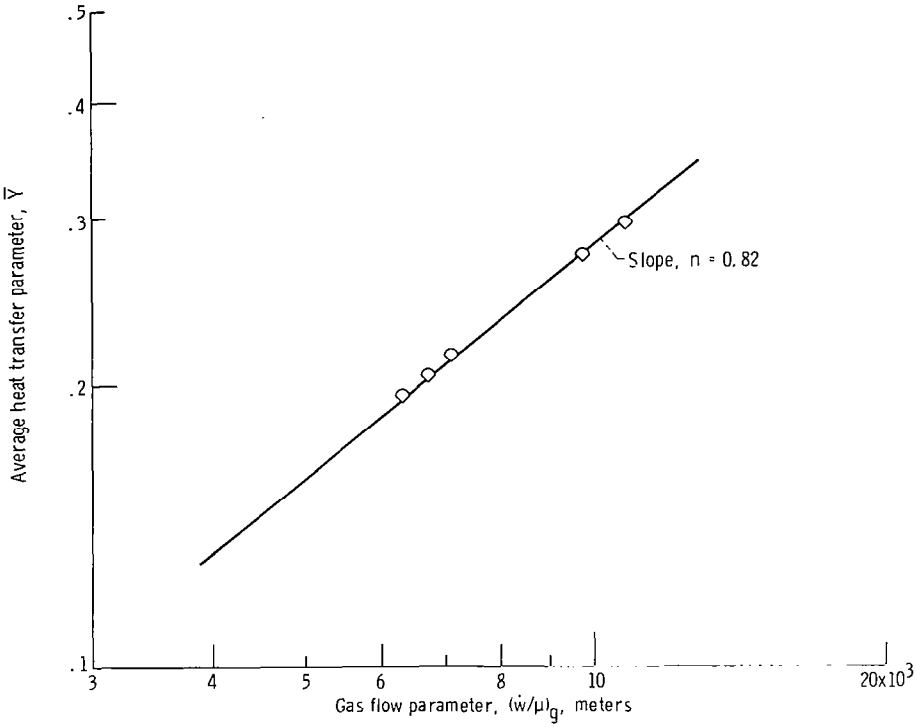

Figure 15. - Representative crossplot showing determination of exponent n of equation (14). Vane coolant flow parameter, $(\dot{w}/\mu)_c$, 2000 meters.

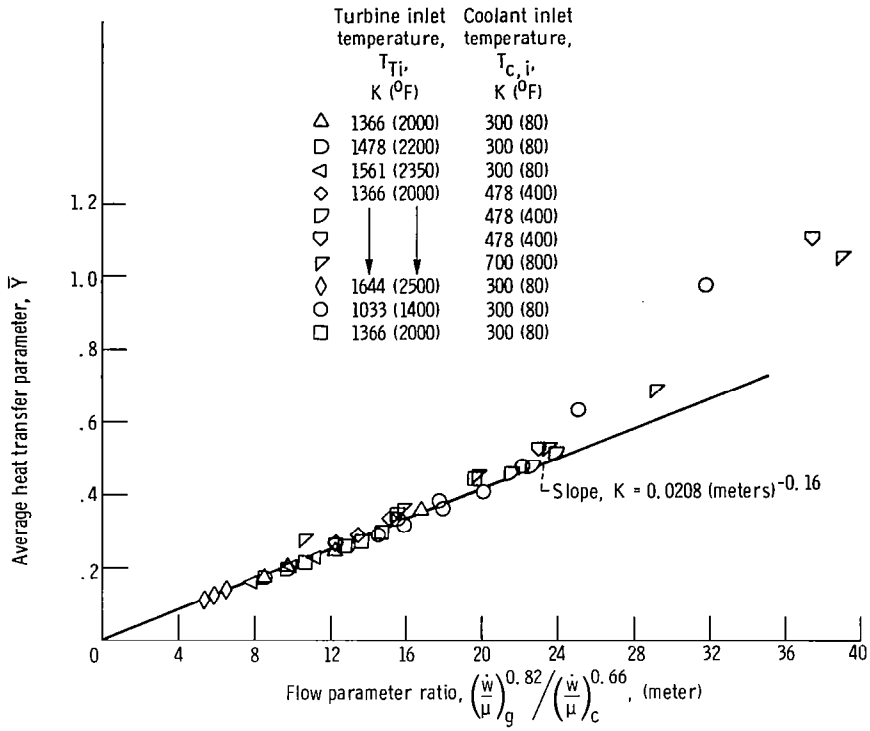

Figure 16. - $\bar{Y}$ correlation from equation (14) for average midspan data.

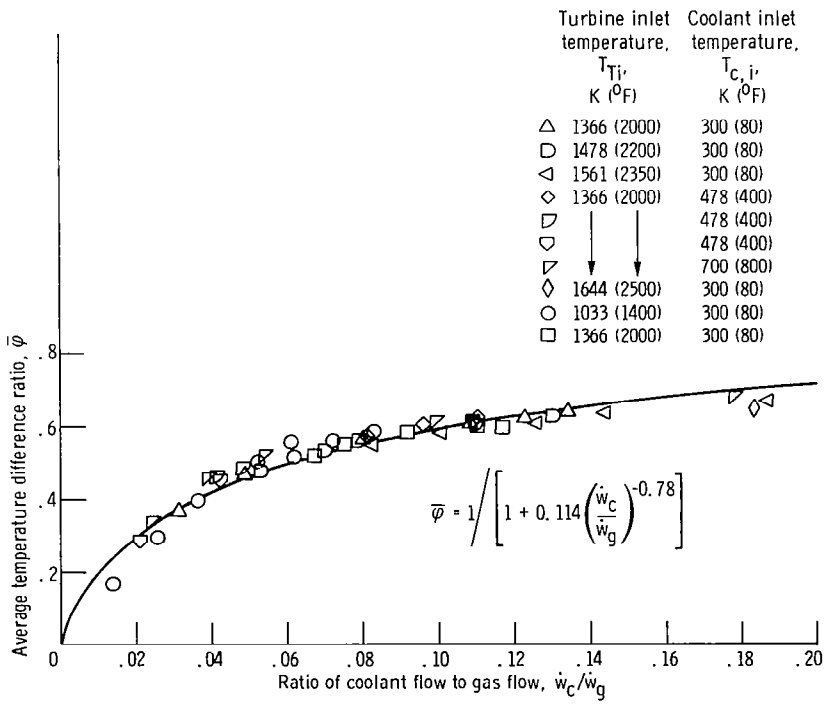

Figure 17. - Average temperature difference ratio correlation for midspan data.

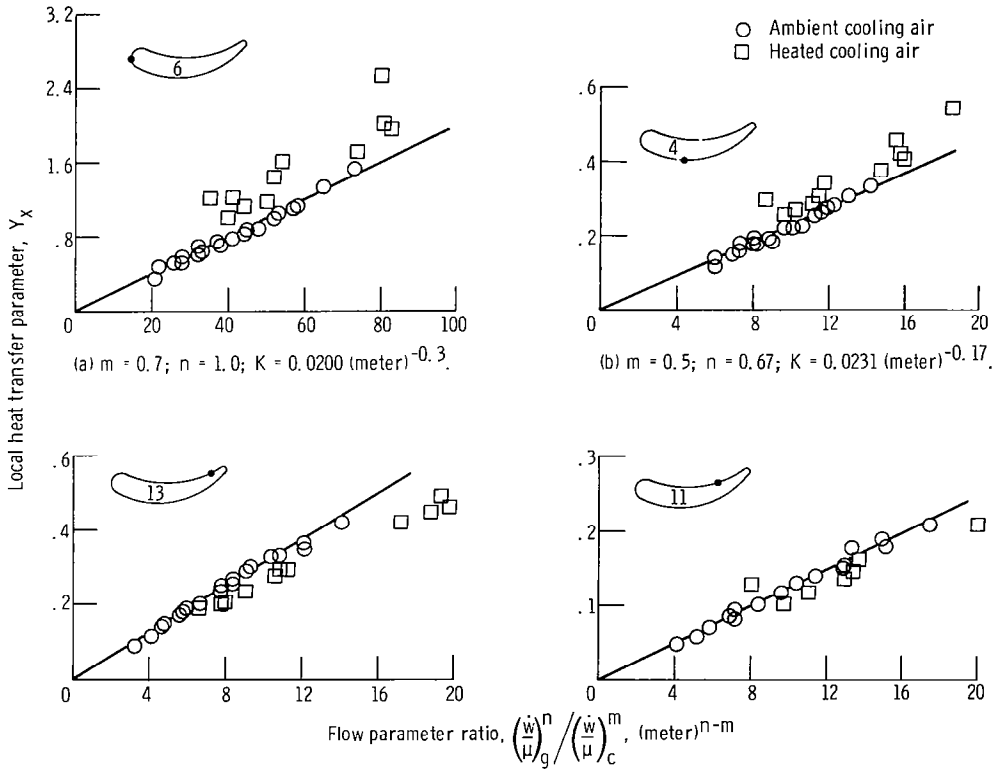

Figure 18. - Local heat transfer correlation for selected midsapn thermocouples using total coolant flow per vane.

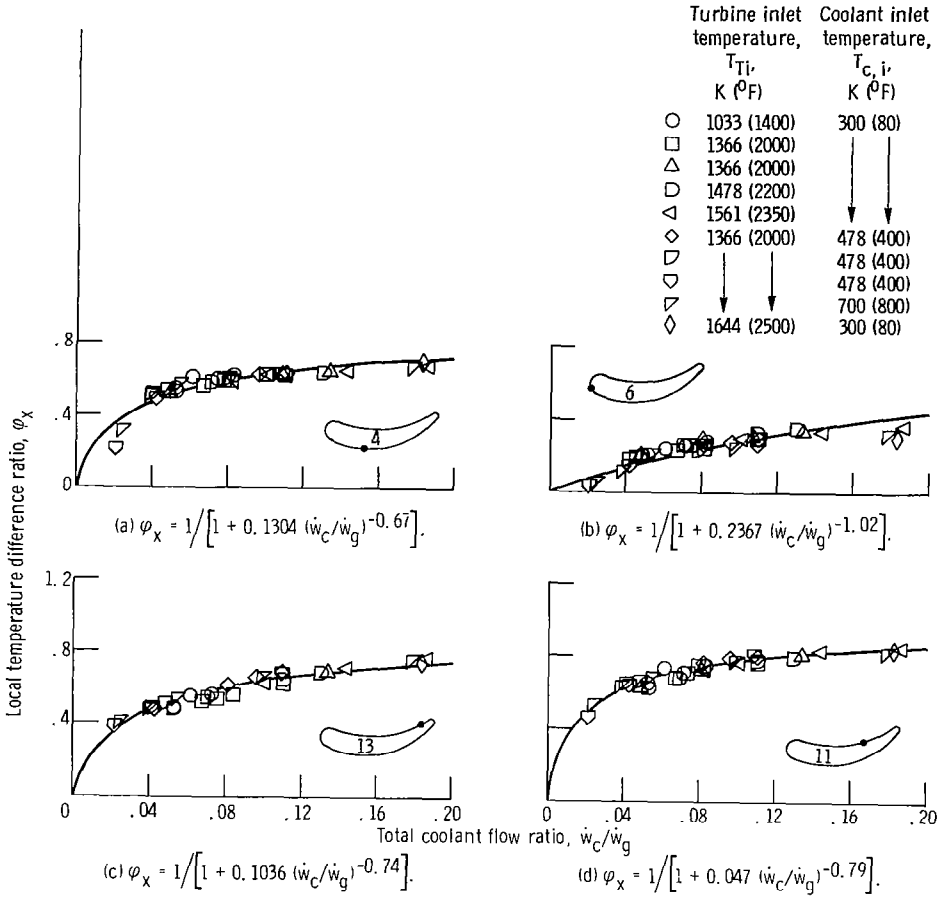

Figure 19. - Local temperature difference ratio for selected midspan thermocouples using total coolant flow.

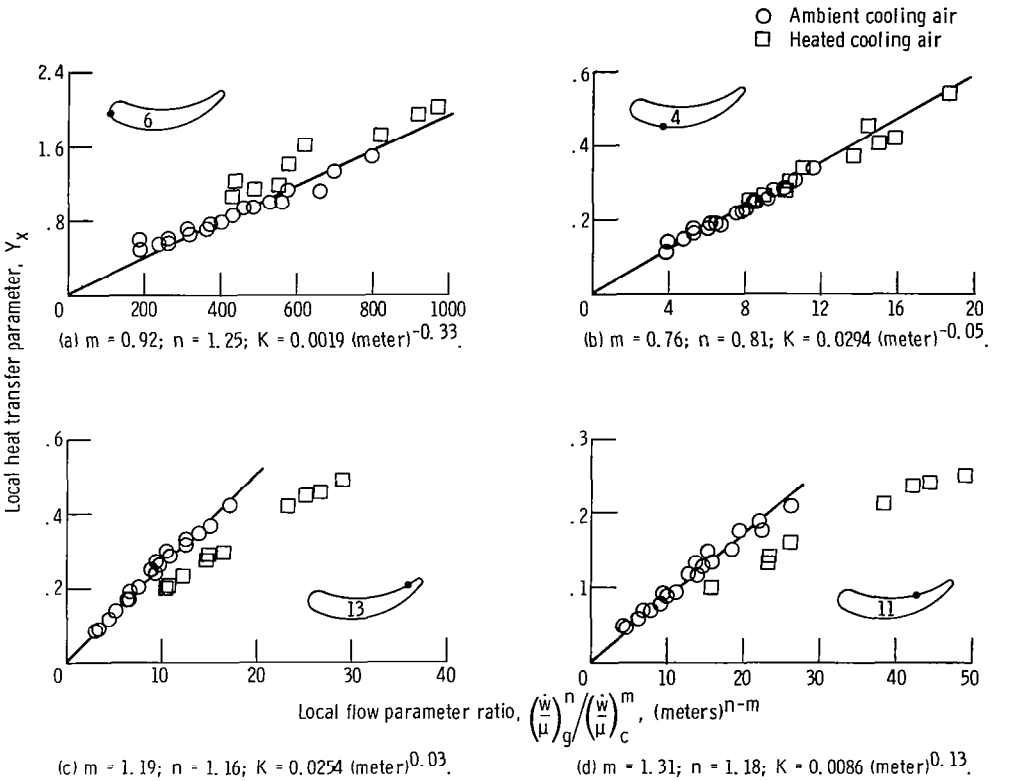

Figure 20. - Local heat transfer correlation for selected midspan thermocouples using exit coolant flow.

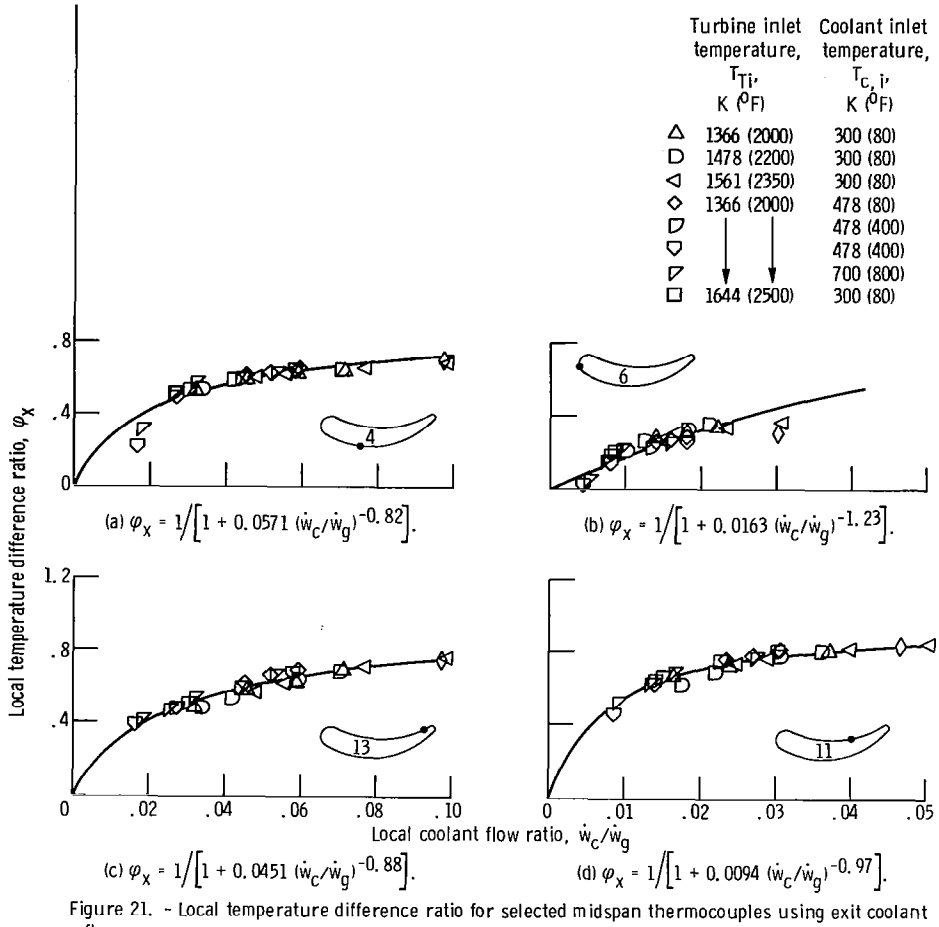

Figure 21. - Local temperature difference ratio for selected midspan thermocouples using exit coolant flow.

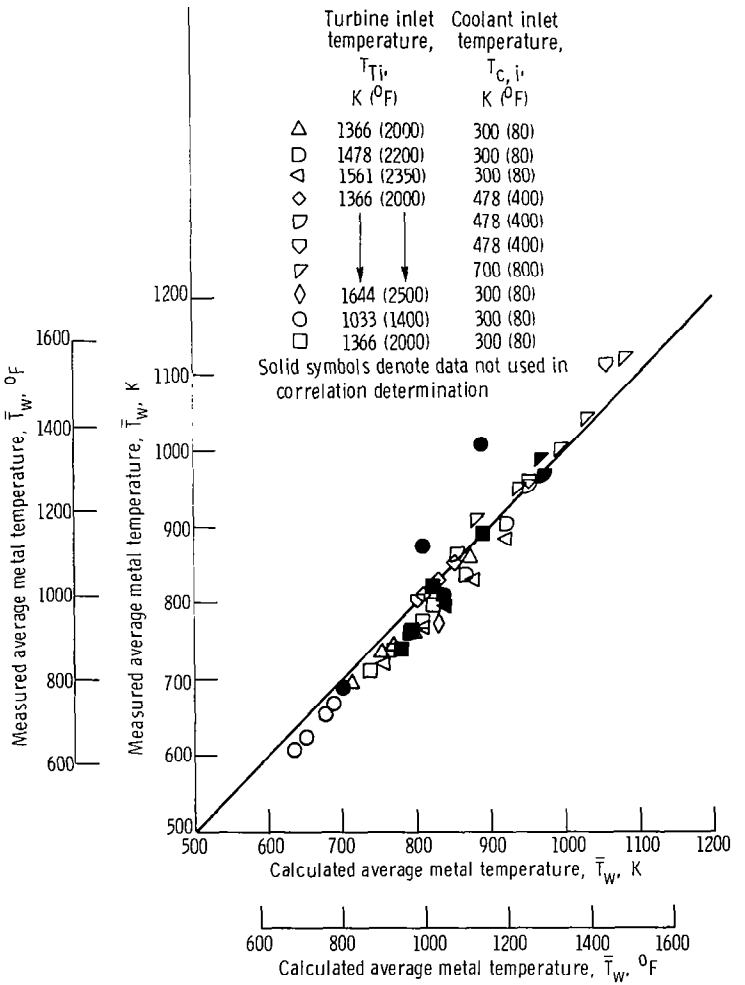

Figure 22. - Comparison of average measured midspan temperatures with average temperatures calculated from $\bar{Y}$ correlation.

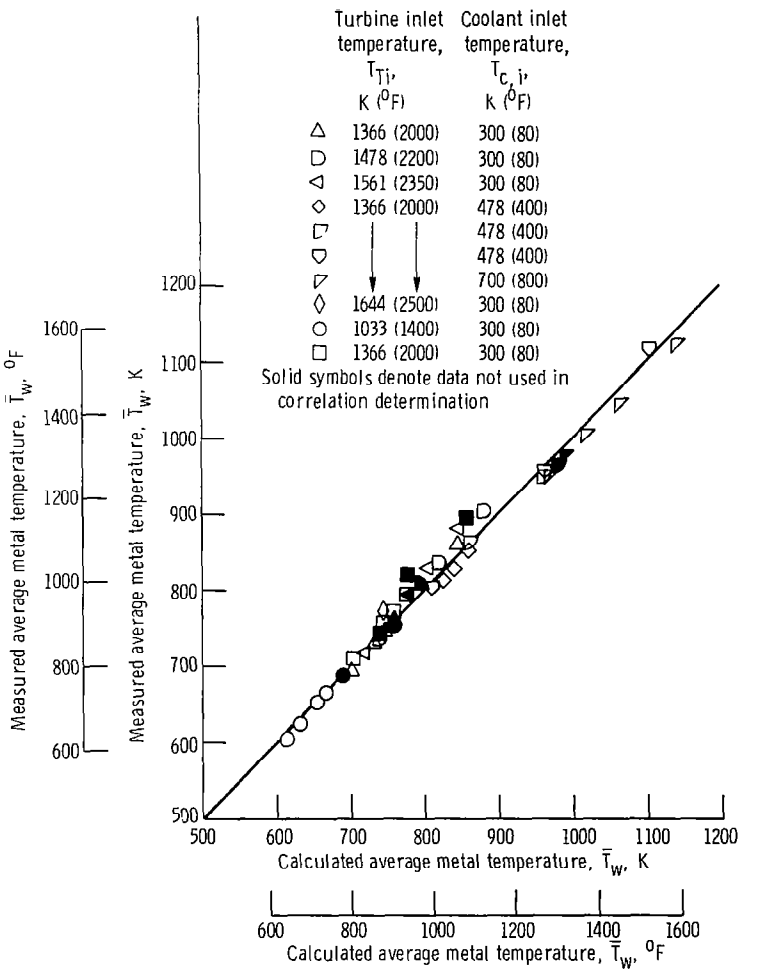

Figure 23. - Comparison of average measured midspan temperatures with temperatures calculated from $\bar{\varphi}$ correlation.

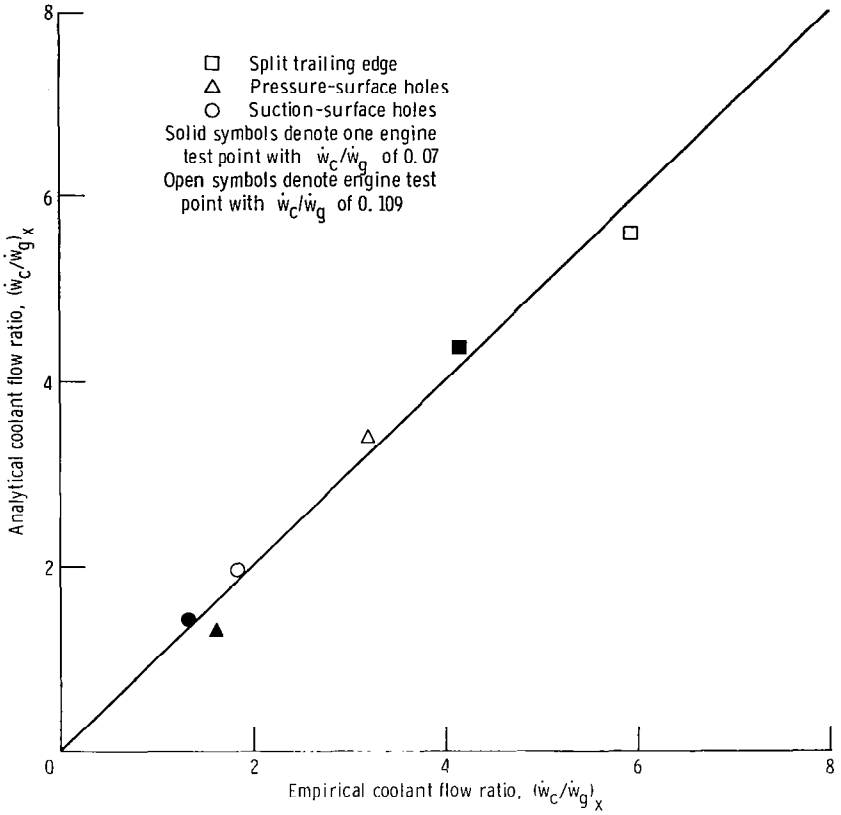

Figure 24. - Comparison of empirical and analytical coolant flow rates through suction- and pressure-surface film cooling holes and split trailing edge.

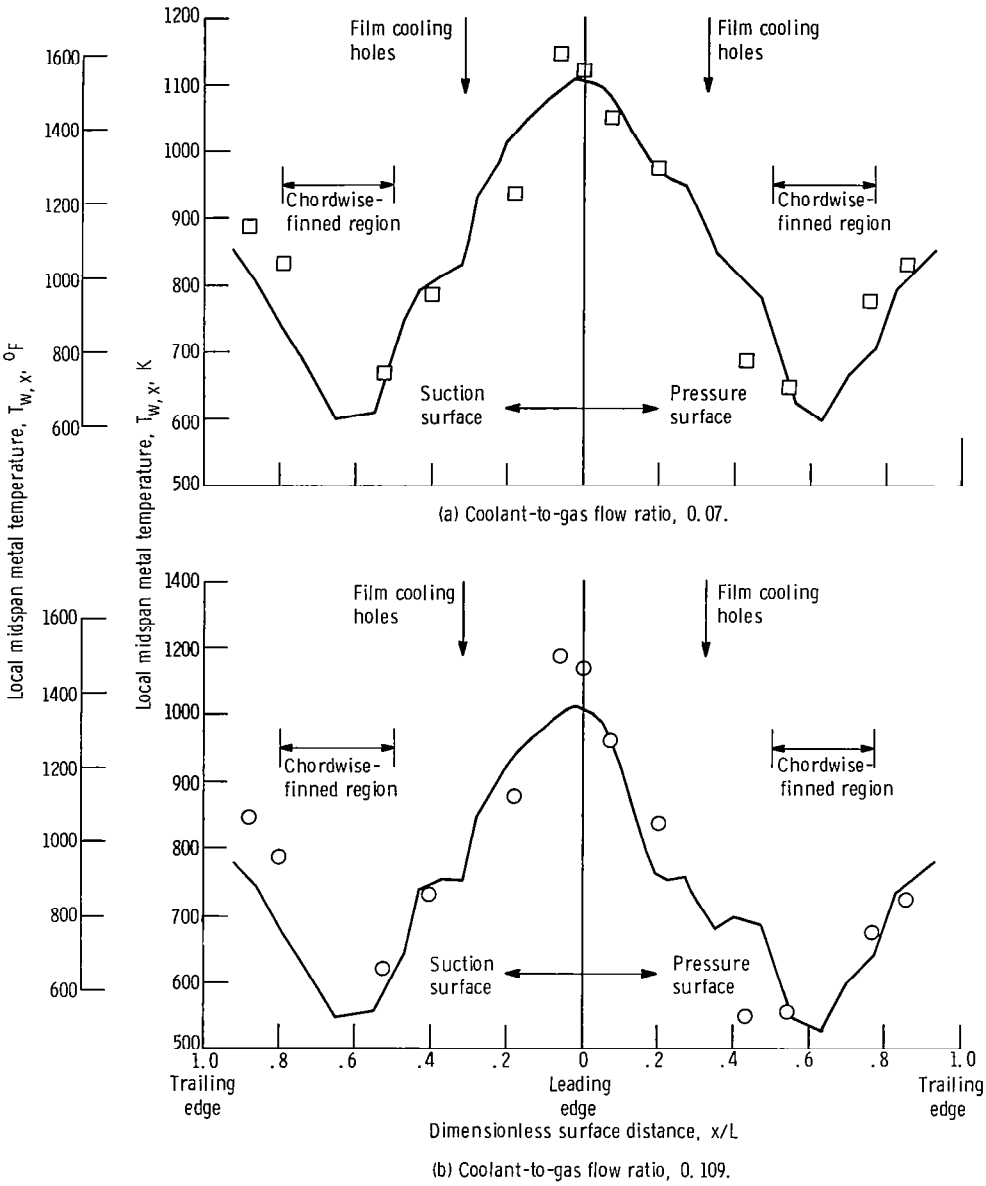

Figure 25. - Comparison between experimental and analytical midspan chordwise temperature distributions for gas temperature of 1478 K (2200^{o} F) and coolant inlet temperature of 300 K (80^{o} F).

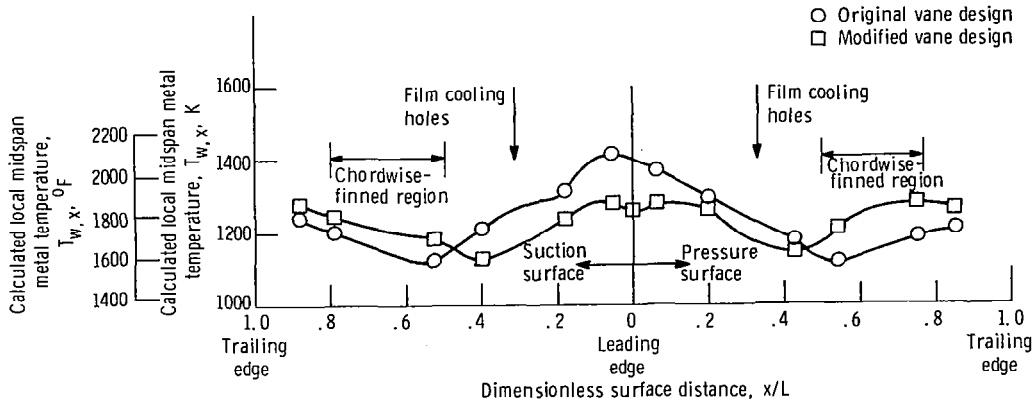

Figure 26. - Calculated chordwise temperature distribution of vane midspan for average gas temperature of 1509 K (2257^{o} F), coolant inlet temperature of 922 K (1200^{o} F), and coolant-to-gas flow ratio of 0.05.

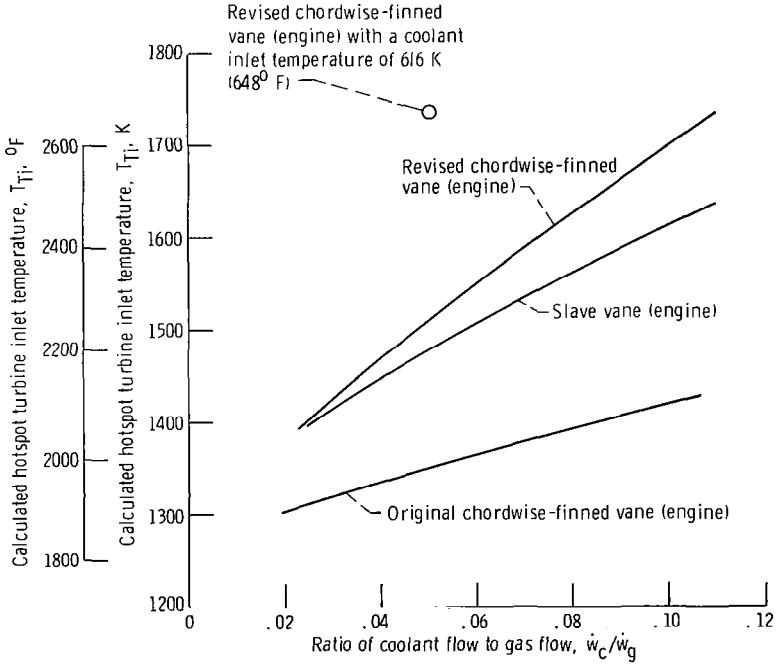

Figure 27. - Calculated hotspot turbine inlet temperature as function of coolant flow ratio for maximum leading-edge vane temperature of 1278 K (1840^{o} F) and coolant inlet temperature of 922 K (1200^{o} F).

"The aeronautical and space activities of the United States shall be conducted so as to contribute . . . to the expansion of human knowledge of phenomena in the atmosphere and space. The Administration shall provide for the widest practicable and appropriate dissemination of information concerning its activities and the results thereof."

—NATIONAL AERONAUTICS AND SPACE ACT OF 1958

NASA SCIENTIFIC AND TECHNICAL PUBLICATIONS

TECHNICAL REPORTS: Scientific and technical information considered important, complete, and a lasting contribution to existing knowledge.

TECHNICAL NOTES: Information less broad in scope but nevertheless of importance as a contribution to existing knowledge.

TECHNICAL MEMORANDUMS: Information receiving limited distribution because of preliminary data, security classification, or other reasons.

CONTRACTOR REPORTS: Scientific and technical information generated under a NASA contract or grant and considered an important contribution to existing knowledge.

TECHNICAL TRANSLATIONS: Information published in a foreign language considered to merit NASA distribution in English.

SPECIAL PUBLICATIONS: Information derived from or of value to NASA activities. Publications include conference proceedings, monographs, data compilations, handbooks, sourcebooks, and special bibliographies.

TECHNOLOGY UTILIZATION PUBLICATIONS: Information on technology used by NASA that may be of particular interest in commercial and other non-aerospace applications. Publications include Tech Briefs, Technology Utilization Reports and Technology Surveys.

Details on the availability of these publications may be obtained from:

SCIENTIFIC AND TECHNICAL INFORMATION OFFICE

NATIONAL AERONAUTICS AND SPACE ADMINISTRATION

Washington, D.C. 20546